TITLE

Modulation of cell differentiation and growth dynamics underlie the shift from bud protection to light capture in cauline leaves.

Le Gloanec C., Gómez-Felipe A., Alimchandani V., Branchini E., Routier-Kierzkowska A-L., Kierzkowski D.*

Institut de Recherche en Biologie Végétale, Département de Sciences Biologiques, Université de Montréal, 4101 Sherbrooke St E, Montréal, QC, H1X 2B2 Canada

*Correspondence: daniel.kierzkowski@umontreal.ca

RUNNING TITLE

Development of the cauline leaf.

ONE SENTENCE SUMMARY

The dual function of the cauline leaf in protection and light capture is achieved during development through a delay of cell differentiation, growth redistribution, and transient growth decrease.

ABSTRACT

Plant organs have evolved into diverse shapes for specialized functions despite emerging as simple protrusions at the shoot apex. Cauline leaves serve both as photosynthetic organs and protective structures for emerging floral buds. However, the growth patterns underlying this dual function remain unknown. Here, we investigate the developmental dynamics shaping cauline leaves underlying their functional diversification from other laminar organs. We show that cauline leaves display a significant delay in overall elongation compared to rosette leaves. Using live imaging, we reveal that their functional divergence hinges on early modulation of the timing of cell differentiation and cellular growth rates. In contrast to rosette leaves and sepals, cell differentiation is delayed in cauline leaves, fostering extended proliferation, prolonged morphogenetic activity, and growth redistribution within the organ. Notably, cauline leaf growth is transiently suppressed during the early stages, keeping the leaf small and unfolded during the initiation of the first flowers. Our findings highlight the unique developmental timing of cauline leaves, underlying their shift from an early protective role to a later photosynthetic function.

INTRODUCTION

Plant lateral organs, such as leaves and flowers, exhibit an incredible diversity of shapes that evolved to ensure their specialized functions and to adapt to their environment. For instance, leaves of different species range from simple to compound with marginal protrusions of varying sizes and shapes (Fukushima and Hasebe, 2014; Vlad et al., 2014). Leaf diversity may also be observed within individual plants as leaf morphology changes during overall plant development – a process called heteroblasty (Nikovics et al., 2006; Yu et al., 2015; Maugarny-Calès and Laufs, 2018; Tang et al., 2023). Furthermore, other flat organs, such as sepals and petals, differ greatly from leaves in their forms and sizes despite deriving from a leaf-like ancestral structure (Bowman et al., 1991; Honma and Goto, 2001; Pelaz et al., 2001).

Regardless of their diversity at maturity, all aerial organs are initiated as simple protrusions at the shoot apical meristem (Hervieux et al., 2016; Echevin et al., 2019; Silveira et al., 2022; Burian et al., 2022). All of them are also suggested to follow a common developmental program after initiation (Burko and Ori, 2013; Runions et al., 2017; Challa et al., 2021; Whitewoods et al., 2020). For instance, studies on leaf diversification revealed common growth behaviors at the global and local scales in both simple and compound leaves (Ori et al., 2007; Kierzkowski et al., 2019). Early quantitative alterations of this shared developmental mechanism are believed to account for the strong differences in final leaf shapes (Kierzkowski et al., 2019; Whitewoods et al., 2020; Wang et al., 2022). How this common program is fine-tuned to achieve specific shapes at maturity is still unclear, but involves precise molecular tuning of patterning, growth, and differentiation (Sablowski, 2015; Kierzkowski et al., 2019; Hamant and Saunders, 2020; Whitewoods et al., 2020; Tang et al., 2023).

Current evidence suggests that the balance between proliferative growth and differentiation is essential in determining the geometry of laminar organs. For instance, the rate of margin differentiation plays a significant role in shaping leaf forms, with delayed differentiation enabling extended patterning and greater leaf complexity (Donnelly et al., 1999; Shani et al., 2010; Bar and Ori, 2014; Vuolo et al., 2018; Kierzkowski et al., 2019). Local auxin maxima at the margin, facilitated by the PIN-FORMED1 (PIN1) auxin transporter, lead to the formation of protrusions such as

serrations or leaflets. However, only undifferentiated cells at the leaf margin are competent to generate auxin maxima and respond to auxin by locally increasing and reorienting growth (Ori et al., 2007; Barkoulas et al., 2008; Bilsborough et al., 2011; Kasprzewska et al., 2015; Ben-Gera et al., 2016; Kierzkowski et al., 2019).

Auxin distribution at the margin has also been suggested to act globally by coordinating cellular growth orientations (i.e., growth anisotropy). In leaves, a distal auxin maximum correlates with global growth orientations converging towards the leaf tip, likely underlying organ shape tapering toward the tip (Jaeger et al., 2008; Kuchen et al., 2012). Conversely, petals exhibit a broader pattern of auxin distribution at the margin, which likely leads to the diverging growth anisotropy underlying its distally broadening shape (Green et al., 2010; Lampugnani et al., 2013; Sauret-Güeto et al., 2013). Thus, auxin plays a critical role in guiding organ formation, although the extent to which it operates locally or globally is still a matter of debate (Bilsborough et al., 2011; Kuchen et al., 2012; Kierzkowski et al., 2019; Whitewoods et al., 2020).

Understanding how plant organs acquire their shapes is essential in the context of their specific functions. For instance, rosette leaves are large organs optimized for photosynthesis, while sepals are small, protecting the internal floral organs during their development (Roeder et al., 2010; Rodriguez et al., 2014; Bielczynski et al., 2017). Cauline leaves are the last few leaves initiated during the meristem transition from the vegetative to the reproductive phase. On one hand, they are efficient photosynthetic organs, contributing to the plant's overall energy production (Su et al., 2011). However, they also serve as protective structures for emerging floral buds during early bolting stages (Pabõn-Mora et al., 2013; Ding et al., 2023). This suggests that the development of these leaves might exhibit characteristics of both rosette leaves and laminar organs of the flower such as sepals (Hempel and Feldman, 1994; Yang and Jiao, 2016). Indeed, when floral identity genes are ectopically expressed in *Arabidopsis*, cauline leaves convert into petal-like organs, while rosette leaf development is unaffected (Krizek and Meyerowitz, 1996; Pelaz et al., 2001). Despite these intriguing features, our understanding of the developmental dynamics of cauline leaves remains unknown.

Here, we characterize the developmental mechanisms contributing to the formation of cauline leaves underlying their functional diversification from rosette leaves and sepals in the model species *Arabidopsis thaliana*. We show that cauline leaves display a strong delay in overall elongation compared to rosette leaves. Through quantitative live imaging, we demonstrate that cauline leaf functional divergence mainly relies on the early modulation of two key components: (1) the rate and distribution of cellular growth, and (2) the timing of cell differentiation. In contrast to rosette leaves and sepals, cell differentiation is strongly delayed in the cauline leaf, allowing extended cell proliferation in the leaf blade, prolonged morphogenetic activity at the margin, and growth redistribution within the developing organ. Importantly, cauline leaf growth is transiently suppressed at very early developmental stages, allowing the leaf to stay small and unfolded during the initiation of the first flowers. Overall, our results demonstrate the unique developmental trajectory of the cauline leaf that underlies the transition from its early protective role to the late photosynthetic function.\

RESULTS

Elongation and unfolding of the cauline leaves are delayed compared to rosette leaves.

Cauline leaves exhibit both vegetative and floral features, as they are initiated from the reproductive meristem (Hempel and Feldman, 1994; Pastore et al. 2011). In contrast to rosette leaves, which have petioles for optimizing light capture, cauline leaves lack petioles but efficiently perform photosynthesis as they are located on the stem, so have direct access to light without being in the shade of other leaves (Fig. 1A-B) (Ding et al., 2023). Furthermore, in their early stages, cauline leaves serve as a protective covering for the inflorescence meristem. This role is analogous to the way sepals shield developing internal organs of flowers (Fig. 1C) (Pabõn-Mora et al., 2013; Ding et al., 2023). The presence of abaxial trichomes on cauline leaves reinforces their protective function (Fig. 1C) (Karabourniotis et al., 2020; Berhin et al., 2021).

We supposed that the dual role of cauline leaves could be reflected in their growth dynamics. Therefore, we characterized the overall elongation of cauline leaves

throughout their development and compared them with first rosette leaves and sepals. We derived two different measures of organ growth. The *absolute* elongation rate (in mm/day) simply reflects the increment of organ length over time (Fig. 1E), like earnings on interest in a saving accounts. The *relative* elongation rate (in %/day) shows how fast the organ elongates in proportion to its previous length (Fig. 1F), analog to the interest rate set by a bank. While the absolute elongation rate is more intuitive than the relative rate, the second measures growth independently from organ size and reflects better cell wall expansion.

The length of first rosette leaves evolved over time following a characteristic sigmoid shape (Fig. 1D), consistent with previous studies on leaf elongation (Cookson and Granier, 2006; Massonnet et al., 2010; Baerenfaller et al., 2015). The speed at which the first leaf elongated peaked at 9 days after initiation (Abs. rate = 1.8 mm/day ± 0.5 SE at 9 DAI) (fig 1E). This peak corresponded to the middle of the S shape, when the first leaf reached about half its final size and experienced a linear growth phase (fig 1D). Splitting our leaf measurements into petiole and blade length (Fig. S1) showed that they followed slightly different sigmoid functions, with the peak of absolute elongation occurring faster in the blade (at 8 DAI) than in the petiole (at 11 DAI), which grew slower but for a longer time (Fig. S1A). By contrast with the measurements of absolute elongation, the relative elongation rate was maximal at the very first days after leaf initiation and decreased rapidly afterwards, reaching around 20%/day at 9DAI (Fig. 1F and Fig. S1C). This fast decrease confirmed previous studies on rosette leaves (Kierzkowski et al., 2019; Le Gloanec et al., 2022; Harline and Roeder, 2023).

Growth dynamics in sepals showed similarities with the first rosette leaves, with maximal values of relative elongation rate in the days just after initiation, followed by a fast decrease (Fig. 1F). Sepals experienced their peak of absolute elongation at 9 DAI, like the first leaves, although with a much lower rate (0.42 day/mm ± 0.09 SE) (Fig. 1E), which explains the smaller length of sepals at maturity (2.6 mm ± 0.2 SE). Ultimately, the low peak of absolute elongation in sepals is due to the slower relative elongation before 9 DAI, preventing the sepal from cumulating length early on (Fig.1D).

Curiously, cauline leaves displayed a very different growth trajectory. Cauline leaves maintained a smaller size than sepals until 13 DAI (Fig.1D), due to a very low absolute elongation rate (Fig.1E). This was caused by a sharp decrease in relative

elongation just after initiation and maintenance of a low relative growth rate (around 25%/day) between 4DAI and 12 DAI (Fig.1F). The first leaves and sepals reached their final size around 13 DAI, at which point they ceased growing both in absolute and relative terms. By contrast, around 13 DAI, the cauline leaf increased it growth rates, reaching a peak in relative elongation rate at 15 DAI (35 %/day ± 5 SE), followed by a peak in absolute elongation at 19 DAI. This delayed secondary growth acceleration compensated for early slow growth, allowing cauline leaves to reach the size of first rosette leaves by 21 DAI (Fig. 1D).

This transition in growth dynamics may reflect the dual function of the cauline leaf, starting with an early protective role followed by acquisition of photosynthetic competency. If this is true, the geometry of the cauline leaves at early developmental stages should resemble that observed in sepal. To test this hypothesis, we monitored the early primordia development using time-lapse imaging starting from 2 days after initiation, when all of them have comparable shape and size (refer to the 'Materials and methods' section for details) (Fig. 1G-I). While the sepal remained curved over the floral bud (Fig. 1I), the first rosette leaf began unfolding around 5 DAI (Fig. 1G), at the same time as its absolute elongation rate started to increase (Fig. 1E). The cauline leaf remained curled towards the floral bud until 12-13 DAI (Fig. 1H), which also coincides with the onset of its faster absolute elongation (Fig. 1E). At their early stages of development, both the first rosette leaf and the cauline leaf could protect their respective meristems. Both organs change their curvature and potentially capture light once entering their fast phase of absolute elongation. The delayed peak of absolute elongation rate for the cauline leaf could help maintain its protective role for an extended period.

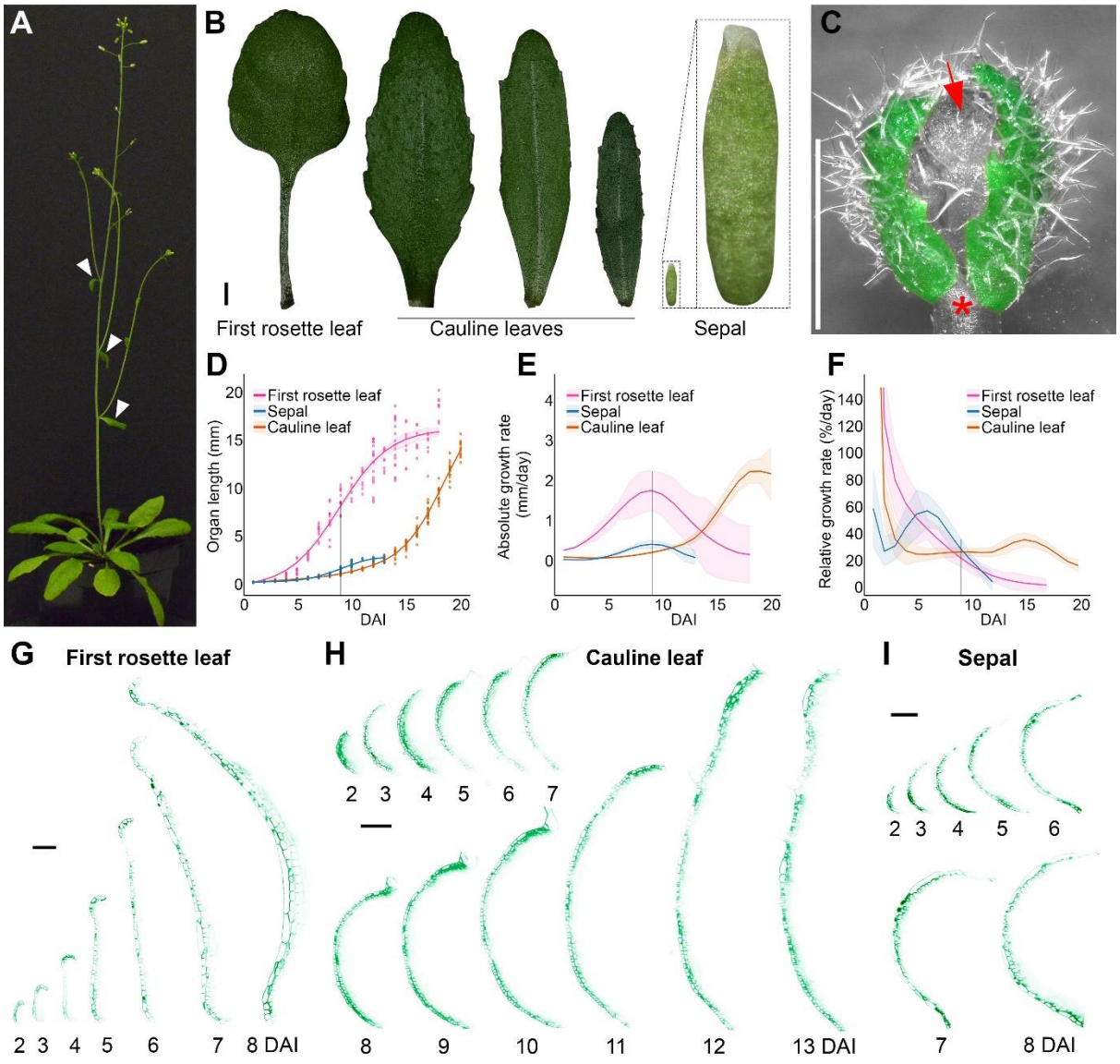

Figure 1. Elongation and unfolding of cauline leaves are delayed compared to rosette leaves. (A) 4-week-old *Arabidopsis thaliana* plant. Cauline leaves are indicated by white arrowheads. (B) First rosette leaf (left), cauline leaves (middle), and sepal (right) at maturity. Inset: close-up view of the sepal. (C) Cauline leaves (colored in green) cover the inflorescence meristem and developing floral buds (red arrow). Star indicates the removed cauline leaf to uncover the initiating flowers. Note the high density of trichomes on the abaxial surface. (D) Organ length plotted against time from initiation to maturity. Points represent independent samples (n=4-21 individual measurements). (E) Organ absolute elongation rate. (F) Organ relative elongation rate, showing a clear resurgence of growth in the cauline leaf at later stages. (D-F) The grey line indicates the time of peak absolute growth rate for the first rosette leaf and the sepal, at 9 DAI. (G-I) Digital, longitudinal sections located in the medial part of the developing first rosette leaf (G), cauline leaf (H), and sepal (I). DAI indicates days after primordium initiation. Scale bars: 1 mm in B-C and 100 µm in G-I. See also Fig. S1.

Cauline leaves display two successive waves of growth at the cellular scale.

We have shown that, similarly to the sepals, in the few days after initiation cauline leaves display slower relative elongation rates than rosette leaves. Subsequently, the relative elongation of cauline leaves accelerates (Fig. 1F), allowing them to catch up in size with rosette leaves (Fig. 1D). To further understand this divergence at the cellular scale, we used our confocal time-lapse imaging pipeline to compute cell area expansion and cell elongation (in relative terms) along the proximodistal and mediolateral organ axes for each cell in the abaxial epidermis using the MorphoGraphX software (Strauss et al., 2022).

Just after initiation (2-3 DAI), relative cellular growth in all organs was fast, with the highest growth rates registered in the first rosette leaf (Fig. 2A-D; Fig. S2). In the cauline leaf and sepal, cells located at the organ tip grew the fastest, while at this stage, cellular growth rates were more homogeneous in the first rosette leaf (Fig. 2). From 3 to 7 DAI, we have observed a progressive decrease in growth rates in all organs. However, this decrease was the most dramatic in the cauline leaf (Fig. 2A-E). During this phase, a clear basipetal (from tip to base) gradient of growth was established both in the first rosette leaf and sepal (Fig. 2A-B and D-E; Fig. S2A, C, D, and F), while in the cauline leaf, cellular growth was very low and homogenous all over the organ (Fig. 2C and D-E; Fig. S2B and E). After 7 DAI, the growth rate further decreased in the first rosette leaf and sepal (Fig. 2A-B and D-E). By contrast, the cauline leaf accelerated its growth from around 7-8 DAI, and this increase continued at least until 13 DAI (Fig. 2C-D). Interestingly, cells located at the tip of this leaf were the first to increase their growth rate, especially along the longitudinal axis of the organ (Fig. 2C-E; Fig. S2B and E). A typical basipetal growth gradient started to be visible in the cauline leaf only from around 11 DAI when cells at the leaf tip ceased expanding (Fig. 2C-E; Fig. S2B and E). Overall, these results show that cellular growth rates at early developmental stages of the cauline leaf are much slower than in the rosette leaves. As a result of this early decrease in growth, the cauline leaf transiently maintains a size in the range observed for sepals. Remarkably, while rosette leaves and sepals progressively slow down growth over their development, the cauline leaf increases its growth at later stages. Thus, two successive waves of growth in the cauline leaf seems to enable its dual function.

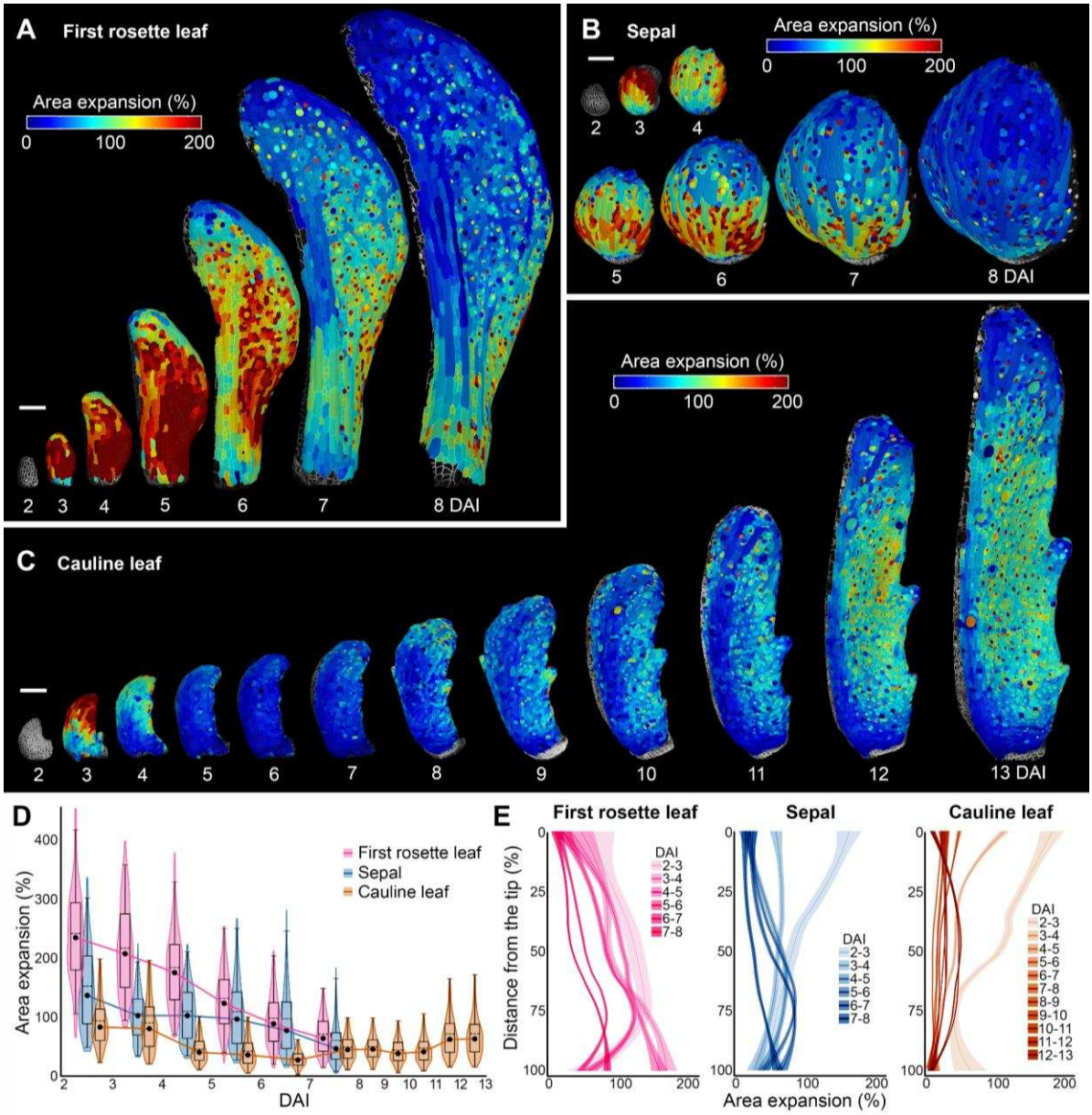

Figure 2. Cauline leaf displays two successive waves of growth. (A-C) Heat maps of area expansion for the *Arabidopsis thaliana* first rosette leaf (A), sepal (B), and cauline leaf (C). (D) Quantifications of area expansion for observed laminar organs. Violin plots and boxplots represent 90% of the values; mean is indicated by a dashed line, median by a black dot connected by a full line (n=810-5827 cells, three independent time-lapse series). (E) Quantifications of area expansion along the proximodistal axis of the first rosette leaf (left), sepal (middle), and cauline leaf (right). Ribbon plots display the normalized distance; the mean is represented by a line, standard deviation by the shaded area (n=58-2626 cells, based on time-lapse series shown in A to C). DAI indicates days after primordium initiation. Scale bars: 100 µm. See also Fig. S2.

248 **Cauline leaf maintains cell divisions during early and late growth phases.**

249 During aerial organ morphogenesis, cells located in fast-growing tissues usually
250 divide more frequently compared to slow-growing areas (Andriankaja et al., 2012;
251 Fox et al., 2018; Zhang et al., 2020; Le Gloanec et al., 2022; Harline and Roeder,
252 2023). Consistently, the basipetal growth decrease in both the first rosette leaf and
253 sepal strongly correlated with the decrease of cell divisions from the organ tip to the
254 base (Fig. 2A, C; Fig. 3A, C). In both organs, cell proliferation activity was first very
255 intensive but quickly decreased at later stages (8 DAI), consistent with a progressive
256 slow down of growth (Fig. 2A, C and D; Fig. 3A, C and D, F). By contrast, the cauline
257 leaf retained its cell proliferative activity until at least 13 DAI, correlating with its
258 prolonged growth phase (Fig. 2B and D; Fig. 3B and E). Surprisingly, cell divisions
259 were also maintained in the cauline leaf during the transition through its phase of
260 slow growth between 4 and 7 DAI (Fig. 2B and D; Fig. 3B and E). Cell divisions and
261 differentiation are intricately linked, and a delay in differentiation often leads to
262 prolonged proliferative activity (Vuolo et al., 2018; Werner et al., 2021; Wu et al.,
263 2021; Gómez-Felipe et al., 2023). This trait of the maintenance of cell division may
264 suggest that cells in the cauline leaf differentiate later than those in sepals and
265 rosette leaves.
266

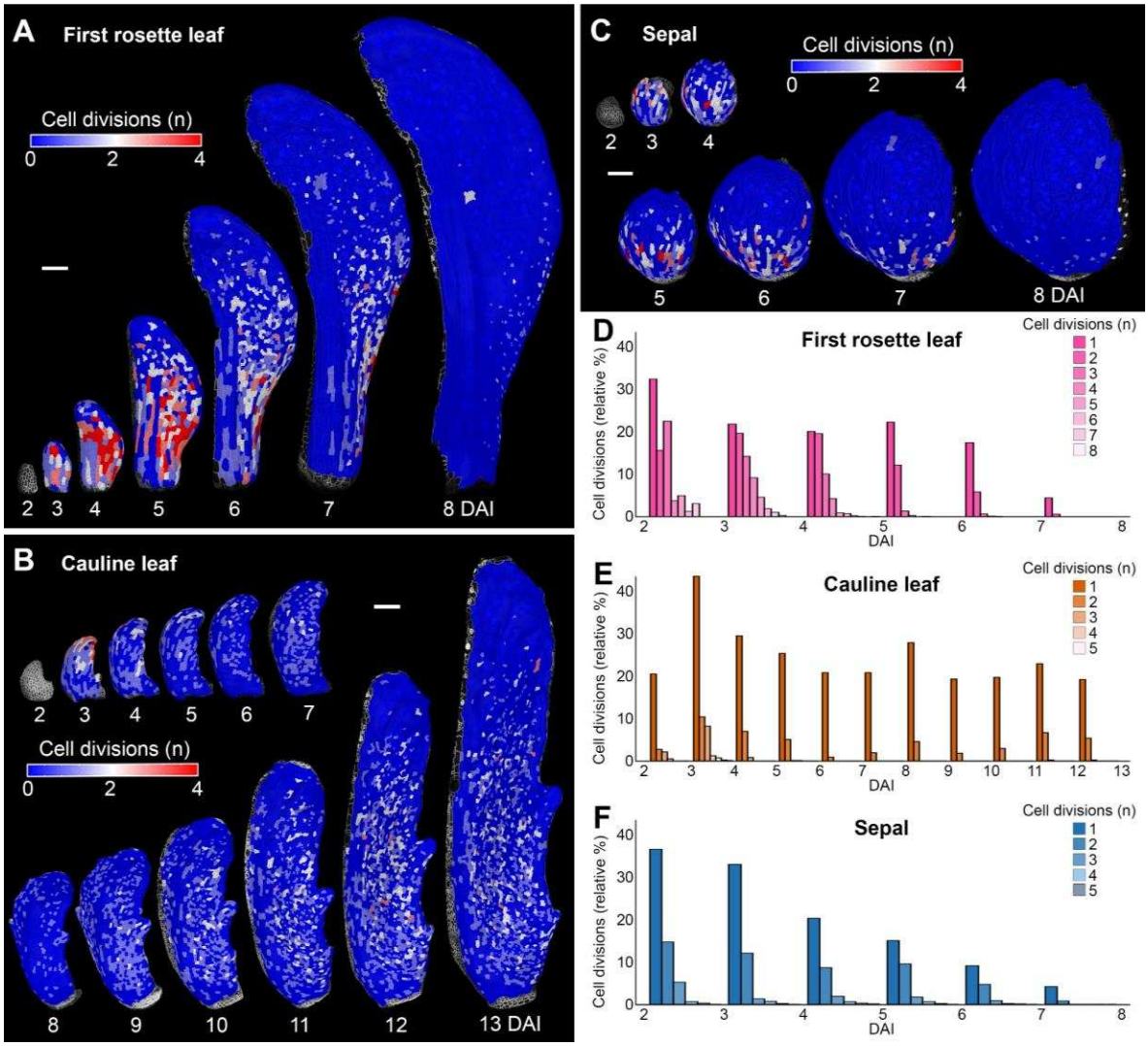

Figure 3. Cauline leaf maintains cell divisions during early and late growth phases. (A-C) Heat maps of cell divisions for the *Arabidopsis thaliana* first rosette leaf (A), cauline leaf (B), and sepal (C). (D-F) Quantifications of cell divisions in first rosette leaf (A), cauline leaf (B), and sepal (C). Barplots represent the relative proportion of cell divisions, normalized by the total number of cells (n=812-5828 cells, three independent time-lapse series). DAI indicates days after primordium initiation. Scale bars: 100 µm.

283 **Cell differentiation is delayed in the cauline leaf.**

284 To verify if cell differentiation is indeed delayed in the cauline leaf, we measured
285 morphological markers of epidermal cell differentiation status such as cell size,
286 stomata distribution, and pavement cell lobeyness (Andriankaja et al., 2012;
287 Rodriguez et al., 2014; Sapala et al., 2018; Le Gloanec et al., 2022). At 8 DAI, the
288 epidermis of first rosette leaves and sepals at 8 DAI consisted of big cells, which
289 often developed extensive lobeyness in the leaf blade and margin or distal region of
290 the sepal (Fig. 4A-C; Fig. S3). At this stage, stomata were already present all over
291 the blade of the first rosette leaf and the entire abaxial epidermis of the sepal (Fig.
292 4D, F-G). By contrast, the cauline leaf epidermis, including the leaf margin, was
293 mostly composed of small isodiametric cells. Only a few cells located at the tip of the
294 first rosette leaf started to increase their size and became lobey (Fig. 4A-C; Fig. S3).
295 Occasionally, some individual stomata could be found in the distal region (Fig. 4E
296 and G), indicating that, at this stage, the cauline leaf is mostly undifferentiated and
297 non-photosynthetic. Stomata spread basipetally through the epidermis only at later
298 stages (from 10 to 13 DAI), suggesting a delay in the establishment of
299 photosynthetic activity in this organ (Fig. 4E). Thus, organ differentiation progresses
300 much faster in both the first rosette leaf and sepal while it is markedly delayed in the
301 cauline leaf.
302

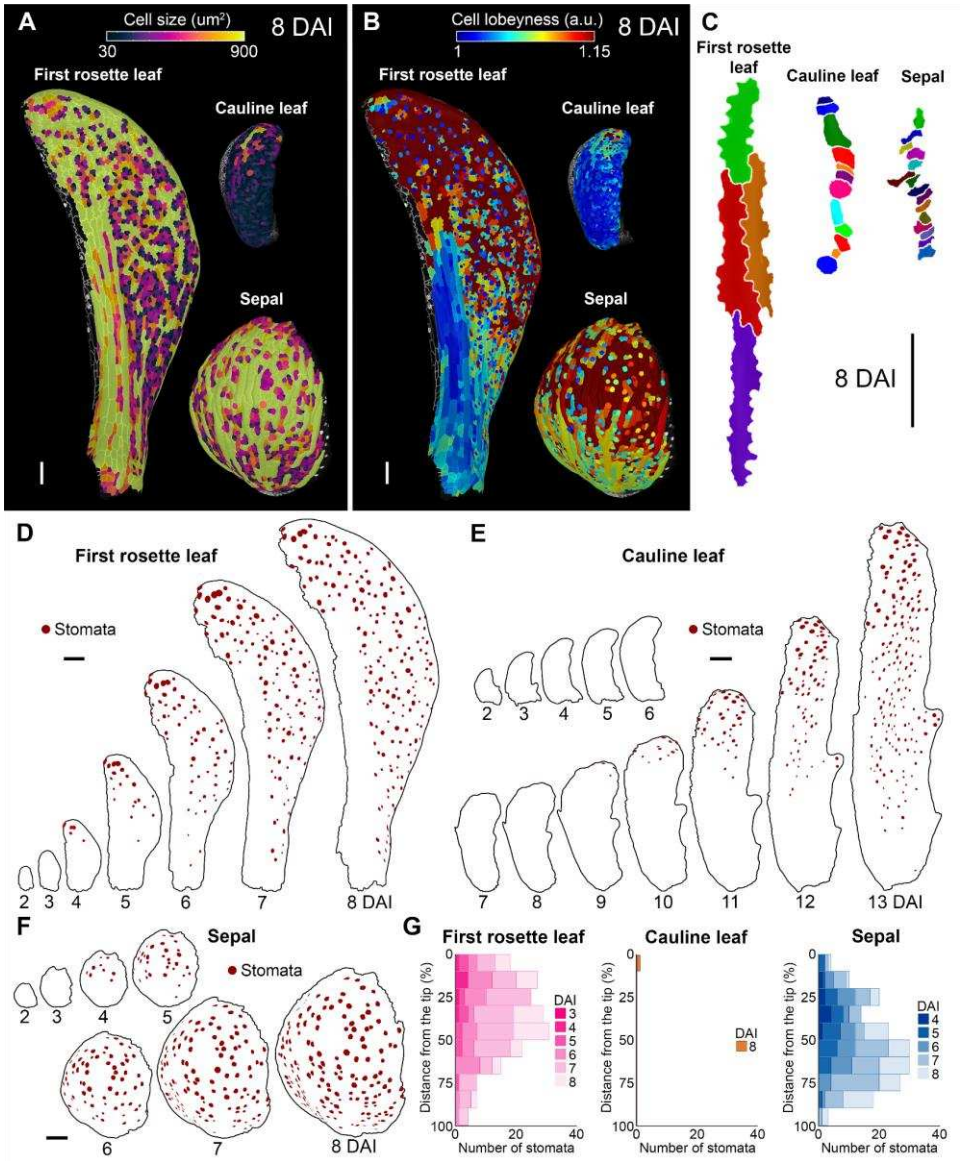

Figure 4. Cell differentiation is delayed in the cauline leaf. (A) Heat maps of cell size in the first rosette leaf (left), cauline leaf (top), and sepal (bottom) at 8 DAI. (B) Heat maps of cell lobeyness in the first rosette leaf (left), cauline leaf (top), and sepal (bottom) at 8 DAI. (C) Geometries of representative cells located at the distal margin of the first rosette leaf (left), cauline leaf (middle), and sepal (right) at 8 DAI. (D-F) Stomata distribution in the first rosette leaf (D), cauline leaf (E), and sepal (F). Stomata marked in brown. (G) Quantification of stomatal distribution as a function of the distance from the tip of the organ for the first rosette leaf (left), cauline leaf (middle), and sepal (right). Bar plots represent the number of stomata. (n=1-189 stomata, based on the time-lapse series shown D to F). DAI indicates days after primordium initiation. Scale bars: 100 μm. See also Fig. S3.

316 **Growth is redistributed in the cauline leaf.**

317 During early development, cauline leaves display a strong delay in cell differentiation
318 compared to the sepals and rosette leaves of the same size (Fig. 4 and Fig. S3). As
319 cell differentiation first occurs in distal portions of these organs, this may lead to an
320 increased contribution of the cells localized at the tip of the early primordium to the
321 final surface of the cauline leaf. Such redistribution of growth, caused by the delay of
322 organ differentiation, has been shown to underlie the development of leaf complexity
323 in Brassicaceae (Kierzkowski et al., 2019).
324 To evaluate this possibility, we computed clonal lineages that developed from cells in
325 early primordia (2 DAI) until all organs reached comparable sizes of around 700 µm
326 (Fig. 5A-C; Fig. S4). Already at this early developmental period, the first rosette leaf
327 displayed smaller clones at the tip, with the marginal cells often stemming from a
328 single cell. In contrast, the basal area grew very fast, producing elongated sectors
329 contributing to over 35% of the organ length at the comparable size of around 700
330 µm (Fig. 5D, G, and J; Fig. S4B, E, and H). Conversely, cells located at the distal
331 region of the early primordium of the cauline leaf grew the fastest and increased their
332 size substantially compared to those at the base (Fig. 5E, H, and K; S4A and D). The
333 contribution of the distal 20% of the primordium surface at 2 DAI increased to around
334 35% of the total organ surface at 10 DAI (Fig. 5E; Fig. S4G). In this respect, the
335 sepal resembled the first rosette leaf, showcasing a greater contribution from basal
336 cells and smaller clones at the tip (Fig. 5F, I, and L; Fig. S4C, F, and I).
337 Interestingly, the growth anisotropy of the clones in the upper half of the first rosette
338 leaf tended to converge toward its tip (Fig. 5N). On the other hand, sectors in the
339 cauline leaf tended to diverge from the main axis of the organ, pointing toward the
340 distal edges of the leaf (Fig. 5N). To a lesser extent, we also observed divergent
341 growth polarities in the sepal, but these sectors were smaller than those in the
342 cauline leaf as they differentiated and ceased their growth early (Fig. 5M). This
343 divergent growth anisotropy of clones in the cauline leaf may result from the
344 maintained morphogenetic activity of its non-differentiated margin, which could act to
345 reorient growth, as previously observed in the petal (Lampugnani et al., 2013;
346 Sauret-Güeto et al., 2013).
347

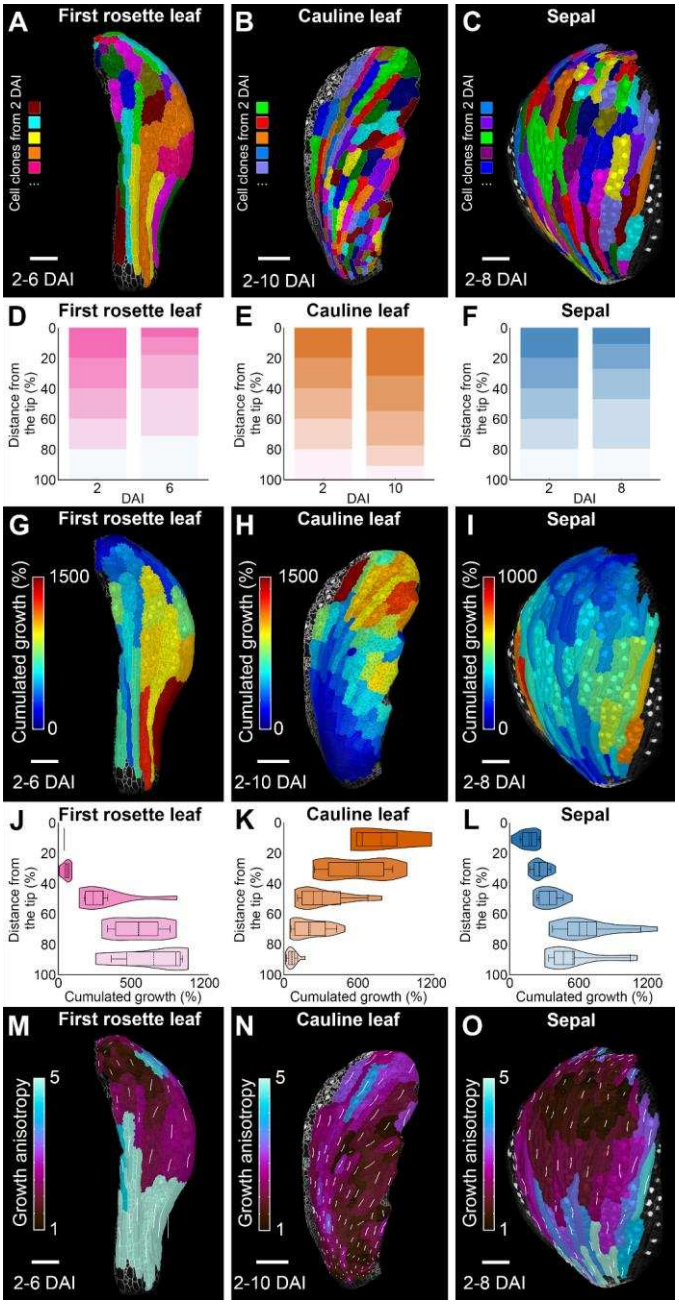

Figure 5. Growth is redistributed distally in the cauline leaf. (A-C) Cell lineage tracing from 2 DAI to the indicated time point (n DAI) in the first rosette leaf (A), cauline leaf (B), and sepal (C) of comparable size. (D-E) Quantification of the contribution of the clones to the length of the organ at n DAI in the first rosette leaf (D), cauline leaf (E), and sepal (F) of comparable size. (G-I) Heat maps of cumulative area expansion (from 2 to n DAI) in the first rosette leaf (G), cauline leaf (H), and sepal (I). (J-L) Quantification of the cumulative area expansion (from 2 to n DAI) in the first rosette leaf (J), cauline leaf (K), and sepal (L). (M-O) Heat maps of growth anisotropy in the first rosette leaf (M), cauline leaf (N), and sepal (O) between 2 and n DAI (comparable size). Stacked histogram represents the relative contribution of equal segments at 2 DAI to the organ length at n DAI. Violin plots and boxplots represent 90% of the values; mean is indicated by a dashed line, median by a line (n=3-7 clones, based on the sample shown in G to I). DAI indicates days after primordium initiation. Scale bars: 100 µm. See also Fig. S3.

Auxin patterning mirrors the differential development of the cauline leaf.

Auxin is a key regulator of cell growth and differentiation (Benková et al., 2003; Ding and Friml, 2010; Di Mambro et al., 2017; Kierzkowski et al., 2019). For instance, auxin maxima at the margin of the leaf and petal are known to locally coordinate cellular growth rates and anisotropy (Barkoulas et al., 2008; Sauret-Güeto et al., 2013; Fox et al., 2018; Kierzkowski et al., 2019; Zhang et al., 2020). To investigate if auxin patterning could underlie the differential growth observed in cauline leaves, we first monitored auxin responsiveness during organ development using the *DR5v2* reporter (Liao et al., 2015). At early stages (~2 DAI), *DR5v2* signal was detected mainly at the tip of the first rosette leaf, and this localization was largely maintained at 4 DAI (Fig. 6A). At later stages (~6 DAI), the *DR5v2* signal started to expand basally throughout the leaf epidermis of the first rosette leaf (Fig. 6A). Interestingly, after the initial tip localization at 2 DAI, *DR5v2* signal extended along the distal edges of the cauline leaf but did not spread throughout the leaf blade at later stages (Fig. 6B). In contrast to both types of leaves, *DR5v2* domain was broader in the distal margin of the sepal from its initiation (Fig. 6C). Like in the cauline leaf, auxin responsiveness was strong in the sepal margin but also spread through the sepal epidermis as in the first rosette leaf (Fig. 6C). A broad marginal distribution of the DR5v2 signal along the margins correlated with divergent growth anisotropy of the clones in both sepals and cauline leaves (Fig. 5). This suggests that auxin accumulation in this domain could locally reorient the growth away from the organ tip as previously observed in petals (Lampugnani et al., 2013; Sauret-Güeto et al., 2013). However, this effect was weaker in sepal as its tip quickly differentiated and stopped growing (Fig. 2B; Fig. 4A-C, and F-G).

Auxin distribution throughout the tissue is mainly regulated by auxin efflux carriers from the *PINFORMED* (*PIN*) family. Therefore, we next monitored the distribution patterns of the *GFP* fusion lines of *PIN1*, *PIN3*, and *PIN7*, which are known to be involved in leaf development (Barkoulas et al., 2008; Guenot et al., 2012; Abley et al., 2016; Mansfield et al., 2018). At early stages (1-2 DAI), *PIN1* was present throughout the epidermis of all three organs (Fig. 6B). This *PIN1* expression was quickly eliminated from the epidermis of the first rosette leaf at around 4 DAI and was restricted to the organ margin in the sepal (Fig. 6B). Interestingly, *PIN1* signal persisted throughout abaxial epidermis of the cauline leaf until at least 6 DAI, and

later was still present in the proximal and lateral regions of the leaf coinciding with the initiation of the marginal serrations (Fig. 6B).

PIN3 was expressed at the tip of the first rosette leaf and sepal from 2 DAI, while it was absent at this stage in the cauline leaf (Fig. 6C). The *PIN3* expression domain quickly (from 4 DAI) expanded basally through the epidermis of the first rosette leaf, while it was restricted to the margin of the cauline leaf (Fig. 6C). The sepal displayed an intermediate *PIN3* expression pattern: first being restricted to the organ margin at 4 DAI, then later expanding throughout the abaxial epidermis at 6 DAI (Fig. 6C). Finally, *PIN7* expression was absent at 2 DAI in all organs, and then quickly expanded through the epidermis of the first rosette leaf and sepal while it was only briefly detected in the medial and proximal regions of the cauline leaf at around 6 DAI (Fig. 6D). Altogether, we found striking differences in auxin patterning that could underlie the differential growth and differentiation patterns between these three laminar organs.

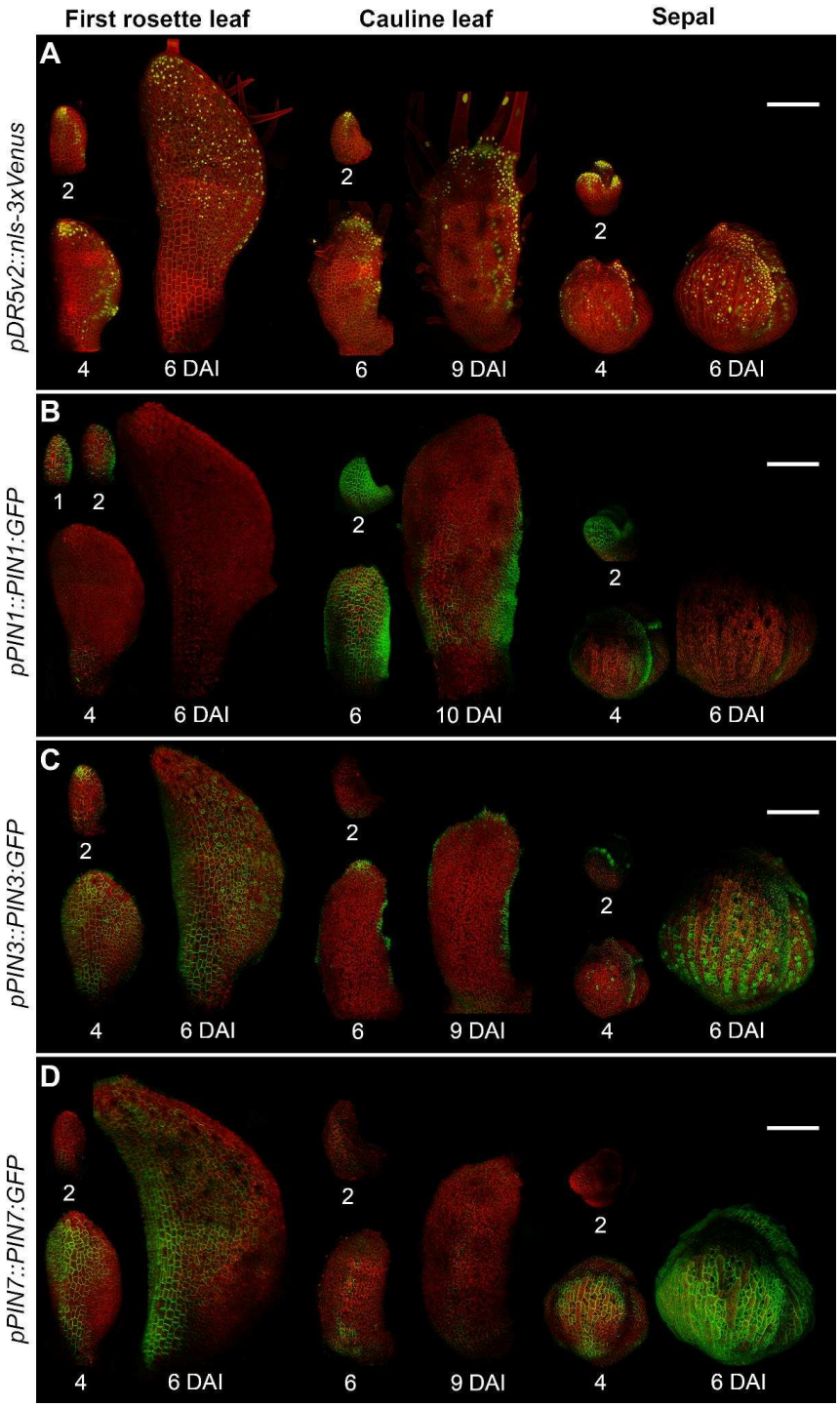

410

411 **Figure 6. Auxin patterning mirrors the differential development of the cauline leaf.** (A)
412 Expression patterns of *pDR5v2::nls-3xVenus* in the first rosette leaf (left), cauline leaf
413 (middle), and sepal (right). (B) Expression patterns of *pPIN1::PIN1-GFP* in the first rosette
414 leaf (left), cauline leaf (middle), and sepal (right). (C) Expression patterns of *pPIN3::PIN3-*
415 *GFP* in the first rosette leaf (left), cauline leaf (middle), and sepal (right). (D) Expression
416 patterns of *pPIN7::PIN7-GFP* in the first rosette leaf (left), cauline leaf (middle), and sepal
417 (right). Autofluorescence and TDT in red; Venus in yellow; GFP in green. DAI indicates days
418 after primordium initiation. Scale bars: 100 µm.

419

DISCUSSION

In this study, we performed a detailed cell-level analysis of development in the cauline leaf and uncovered what sets it apart from other aerial organs, such as rosette leaves and sepals. We revealed that two main factors drive its functional distinction: (1) the timing of cell differentiation and (2) the speed and distribution of cellular growth. More specifically, cauline leaves experience a strong delay in cell maturation (Fig. 3; Fig. 7). Consequently, they display an extended period of proliferative activity and a global redistribution in growth towards the more distal parts of the organ (Fig. 2; Fig. 4; Fig. 5; Fig. 7). Remarkably, cauline leaves undergo a transient phase of slow expansion followed by a resumption of rapid growth (Fig.1; Fig. 2).

Tuning cell differentiation is known to be critical for shaping plant organs (Efroni et al., 2010; Rodriguez et al., 2014; Alvarez et al., 2016). For example, delaying the transition from cell proliferation to cell maturation by class I Knotted-like Homeobox (*KNOXI*) genes has been shown to be a key component allowing the development of complex leaf shape (Hay and Tsiantis, 2006; Barth et al., 2009; Nakayama et al., 2014; Kierzkowski et al., 2019; Wang et al., 2022). Interestingly, the expression of *KNOXI* genes leads to a redistribution of growth within the organ, resulting in an increased contribution of distal organ regions to the final organ shapes (Kierzkowski et al., 2019). A similar mechanism has been observed in floral organs such as petals, where a broad distal region develops only when cell differentiation is suppressed by the action of *JAGGED* (*JAG*), which downregulates cell cycle inhibitors (Schiessl et al., 2012). Consistently, the delay of cell differentiation in cauline leaf also correlates with a greater contribution of its distal region to the organ surface (Fig. 5), suggesting that delaying the basipetal progression of cell differentiation may be a general mechanism for how plant organs change their proportions.

Interestingly, the transition from juvenile to adult phases in *Arabidopsis* leaves controlled by SQUAMOSA-promoter binding protein-like (*SPL*) genes has also been found to influence leaf morphology by delaying maturation while promoting growth and cell divisions in an age-dependent manner (Schwarz et al., 2008; Xu et al., 2016; He et al., 2018; Tang et al., 2023). *SPL10* has been shown to target genes

involved in the cell cycle regulation, such as *CYCLIN D3;3* and *A2;3* (*CYCD3;3* and *CYCA2;3*) (Tang et al., 2023). As the cauline leaf marks the extremity of the heteroblastic series, the regulation of *SPL*s may underlie the strong delay in cell maturation observed in this organ. Indeed, repression of *SPL10* genes results in noticeable morphological changes in the cauline leaf, converting its shape towards the rosette leaf, including the development of a broader leaf blade (Shikata et al., 2009; Huijser and Schmid, 2011).

Auxin is known to accelerate cell differentiation and growth in *Arabidopsis* rosette leaves (Challa et al., 2019; Kierzkowski et al., 2019; Zhang et al., 2020). Here, we found that faster progression of the overall cell differentiation correlates with an early basipetal spread of auxin sensing through the abaxial epidermis of both sepal and first rosette leaf (Fig. 6). This early spread was associated with the elimination of the *PIN1* auxin efflux carrier from the abaxial epidermis that was quickly replaced by the basally progressing expression of *PIN3* and *PIN7* transporters (Fig. 6). By contrast, we observed a prolonged expression of *PIN1*, and the corresponding restriction of auxin sensing to the margin of the cauline leaf (Fig. 6). This data is consistent with recent results from the gynoecium where changes in *PIN*-mediated polar auxin transport were tightly correlated with the onset of cell differentiation in the style (Gómez-Felipe et al., 2023). Thus, modulation of active polar auxin transport may be broadly involved in controlling the basipetal progression of cell differentiation through lateral organs in plants.

Our findings indicate that marginal cells in rosette leaves undergo early differentiation, while in the cauline leaf, cells remain smaller and mainly undifferentiated (Fig. 4). *PIN3* expression expanded during the early stages of the cauline leaf development and coincided with broad redistribution of *DR5v2* signal through the distal margin (Fig. 6). Such *PIN3*-mediated auxin redistribution at the margin has been suggested to coordinate growth orientations in the petal, leading to the creation of the divergent growth polarity in its distal end (Lampugnani et al., 2013; Sauret-Güeto et al., 2013). A similar mechanism seems to operate during the early development of the cauline leaf, where growth in the distal blade is oriented toward its margin (Fig. 5). However, such reorientation of growth in the cauline leaf and petal may occur only because of their general delay in cell differentiation in the

epidermis. In sepals, despite broad distribution of *PIN3*, higher accumulation of DR5v2 signal, and smaller cells at the margins, the early onset of basipetal gradient of differentiation in the epidermis quickly reduces the ability to reorient growth toward the margin.

Interestingly, both petal and cauline leaves are bent toward the inside of the flower for a prolonged period and do not quickly unfold like rosette leaves (Fig. 1) (Smyth et al., 1990; Pabõn-Mora et al., 2013). The delay of differentiation combined with the distally localized growth in the early cauline leaf may help to prevent its early unfolding. While the mechanism underlying this change in curvature remains unclear, current evidence suggests that it likely involves differential growth between both organ surfaces (Zhao et al., 2020; Jiao et al., 2021; Yadav et al., 2023). Such growth asymmetry might be controlled by the differential gene expression during the establishment of organ polarity. For instance, *ARF3* or *ETTIN* marks the abaxial side of the incipient leaf primordia and was shown to regulate the elongation of the valve tissue in the gynoecium (Andres-Robin et al., 2018; Burian et al., 2022).

In contrast to rosette leaves, which exhibit a sigmoid growth curve influenced by leaf age (Cookson and Granier, 2006; Baerenfaller et al., 2015), cauline leaves display a distinct pattern: an initial rapid decline in growth rates, followed by a surprising growth resumption (Fig. 1; Fig. 2). Although genetically induced delay of cell differentiation is known to cause decrease in growth rates (Kierzkowski et al., 2019; Wang et al., 2022), the temporary slow down in cell expansion followed by an acceleration of growth has never been documented during normal development of *Arabidopsis* leaves. However, such growth dynamics is characteristic for some floral organs, such as petals and filaments of the stamen (Smyth et al., 1990; Sauret-Güeto et al., 2013; Silveira et al., 2022). The genetic factors driving late-stage acceleration in growth remain unclear but phytohormones such as auxin, jasmonate, and gibberellins are believed to be key players, especially in the growth resumption of the stamen (Nagpal et al., 2005; Reeves et al., 2012; Cecchetti et al., 2013; Huang et al., 2020; He et al., 2023). Given the genetic proximity between cauline leaves and floral organs (Krizek and Meyerowitz, 1996; Pelaz et al., 2001), it would be interesting to investigate whether similar mechanisms govern cauline leaf development to help fulfill its dual function.

Finally, growth cessation also occurs during bud dormancy when the shoot apex inhibits axillary bud development - a phenomenon known as apical dominance (Junttila and Hänninen, 2012; Bredmose and Costes, 2017). Cauline leaves are initiated before the onset of the dormancy of the axillary buds, thus molecular signals controlling apical dominance and bud dormancy may also be involved in the transient partial inhibition of growth and subsequent growth resumption in these leaves (Rinne et al., 2011; Cooke et al., 2012; Liu et al., 2016; Salem et al., 2018; Hao et al., 2019; Martignago et al., 2020).

Our quantitative study brought new insights into the crucial role of temporal dynamics in orchestrating proper morphogenesis and functional maturation in laminar organs in plants. It provides a solid framework to investigate the molecular mechanisms underlying the development of the cauline leaf, enabling its transition from protection to photosynthesis. Such an approach could offer a deeper understanding of how these organs, originating from a common ancestor, have evolved to fulfill distinct functional roles.

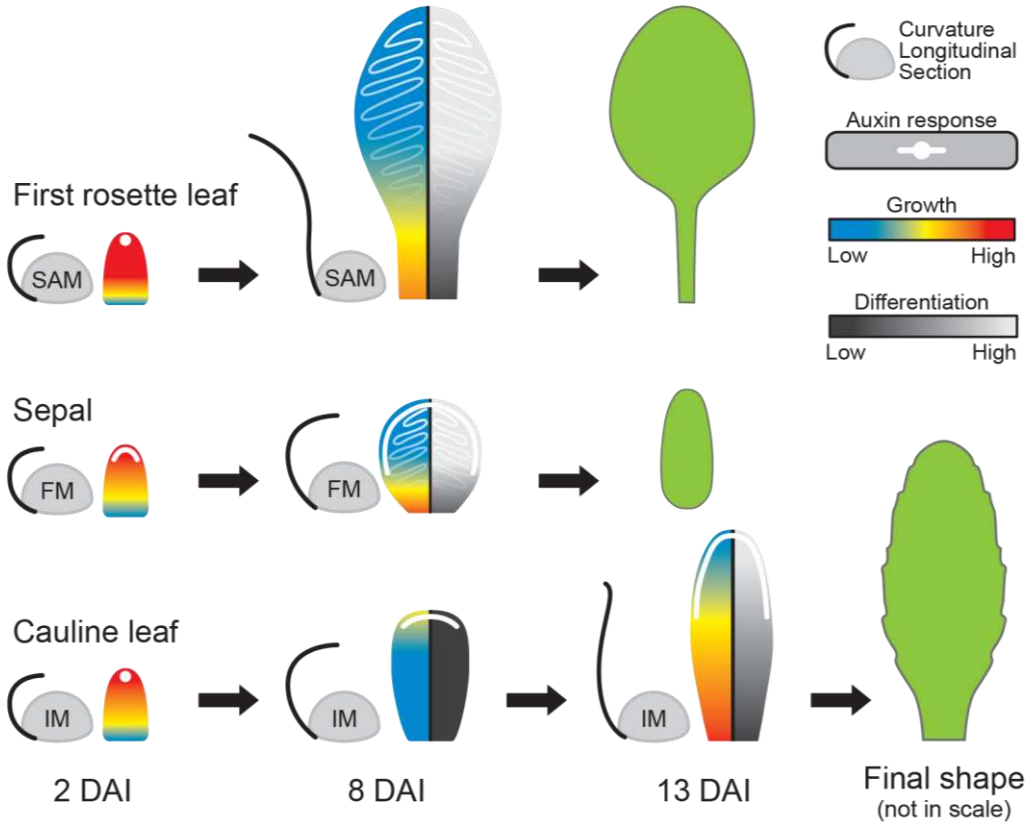

Figure 7. Quantitative modulation of growth and differentiation underlies cauline leaf development. Schematic representation of *A. thaliana* first rosette leaf, cauline leaf, and sepal shapes. Growth rates are depicted through blue-red gradients and differentiation rates by black-grey gradients, while the white color indicates the temporal distribution of auxin at specific developmental time points. All organs initiate as finger-shaped, fast-growing primordia that are curled toward meristems. In the first rosette leaf, growth and differentiation gradients are rapidly established, accompanied by auxin redistribution throughout the epidermis, and the leaf unfolds quickly. Growth and differentiation gradients in the sepal also rapidly progress; auxin is redistributed throughout the leaf margin and the epidermis, and the organ remains curled toward the flower. In contrast, the cauline leaf undergoes a transient slow-growing phase when cells remain undifferentiated, and auxin is retained at its distal margin. During this slow-growing phase, the cauline leaf stays curled toward the inflorescence. At late stages, growth rates increase again, gradients of growth and differentiation start to progress, and the leaf unfolds. DAI indicates days after primordium initiation.

MATERIAL AND METHODS

Plant material and growth conditions

The following *Arabidopsis thaliana* transgenic lines were used in this study: *pUBQ10::myr-YFP* (Willis et al., 2016), *pUBQ10::PM-TDT* (Melnyk et al., 2015), *pDR5v2::nls-3xVenus* (Liao et al., 2015), *pPIN1::PIN1-GFP* (Heisler et al., 2005), *pPIN3::PIN3-GFP* (Žádníkova et al., 2010), and *pPIN7::PIN7-GFP* (Belteton et al., 2018). All lines are in the Col-0 background except for the DR5 reporter line, which is in the Columbia/Utrecht background. *pDR5v2::nls-3xVenus* was crossed with *pUBQ10::PM-TDT* and observed in the 5th generation. Seeds were stratified in the dark for two days at 4°C to synchronize germination. Plants were grown on soil in a growth chamber under long-day conditions (16h/8h light/dark period, 95 $\mu mol.m^{-2}.s^{-1}$) at 22 ± 1°C with 60-70% relative humidity.

Quantification and statistical analysis

Python scripts were used to generate plots in Figures 1D, 2D, F, H, 3, and 5, and Supplemental Figures 2 and 3, while R scripts were used for Figures 2E, G, I, and 4. Violin plots represented value distributions, encompassing 90% of the data. Ribbon plots indicated the mean with shaded areas representing standard deviations. Stacked histograms assessed the relative contribution of equal segments at 2 DAI during specific time points. Barplots represented the relative proportions of each value per time point using bars.

Organ-scale time-lapse imaging and length measurements

Plants cultivated under the above-described conditions were standardized by selecting individuals of comparable sizes. Individual first rosette leaves were excised starting from 2-day-old plants every 24 h. Cauline leaves were dissected starting from 10-day-old plants every 24 h. Three successive cauline leaves from the same plant were imaged. Abaxial sepals of the first flowers were imaged every 24 h starting from 20-days-old-plant. All images were acquired using a Keyence digital microscope model VHX-970F. The lengths of all organs were measured using Fiji following the abaxial surface from the base to the tip of the organ (Rasband et al., 1997-2018).

591

592 **Analysis of organ-scale growth**

593 Time-lapse measurements of organ length from the developing leaves, cauline
594 leaves, and sepals were fitted to an analytical function $L(t)$. A sigmoid function
595 $L(t) = \frac{a}{1+e^{(-c(t-b))}} + d$, where t is the time in days, was fitted to the rosette leaf, its
596 blade and petiole (Fig. 1D; Fig. S1) using *optimize.curve_fit* from SciPy. Splines
597 were used to fit the length of the cauline leaf and sepal using *interpolate.BSpline* and
598 *interpolate.splerep* with smoothing condition $s = 0.1$ from SciPy. Absolute growth
599 rate (AGR), defined as the first derivative over time of the fitted function $L(t)$, was
600 calculated using the *gradient* function in NumPy (Fig. 1E). Relative growth rate
601 (RGR) in %/day was defined as $R(t) = 100\, e^{(r(t)-1)}$, where $r(t) = \frac{ln\left(\frac{L(t)}{L(t-\Delta t)}\right)}{\Delta t}$, and was
602 calculated from the fitted $L(t)$ function (Fig. 1F).

603

604 **Confocal time-lapse imaging**

605 For cauline leaf, cotyledons and older leaf primordia were removed using fine
606 tweezers or an injection needle from two-week-old plants to expose the initiating
607 cauline leaf primordium. The dissected plants were placed horizontally in Ø60 mm
608 Petri dishes filled with ½ Murashige and Skoog (MS) medium, supplemented with
609 1.5% agar, 1% sucrose, and 0.1% Plant Protective Mixture (Plant Cell Technology).
610 Plants were immersed in water containing 0.1% PPM for imaging. For each replicate,
611 at least half of the abaxial leaf surface was imaged at 24 h intervals for up to 10
612 days. Between imaging, water was removed, and samples were cultured in vitro
613 under standard long-day conditions in a growth chamber. The images shown in
614 Figures 2A, 3A, and 4D and Supplemental Figures S2A, D, and S3A, D are derived
615 from two independent overlapping series (2-7 DAI and 8-13 DAI). Time-lapse
616 imaging of juvenile leaves and sepals was previously described (Hervieux et al.,
617 2016; Le Gloanec et al., 2022).
618 All confocal imaging was performed with an LSM800 upright confocal microscope
619 using a long-distance water-dipping objective (AP 40X/1.0; Zeiss). Excitation was
620 performed using a diode laser with 488 nm for YFP, GFP, Venus, and 561 nm for
621 TDT and autofluorescence. Images were collected at 500-550 nm for YFP, GFP, and
622 Venus, 560-650 nm for TDT, and 600-700 nm for autofluorescence. Confocal stacks

were acquired at 512x512 resolution and 16-bit image depth, with 0.5-2 µm distance in Z-dimension. Imaging was performed with the same confocal settings for each fluorescence marker line. For samples larger than the field of view, multiple overlapping stacks were obtained and later stitched together using MorphoGraphX (Barbier de Reuille et al., 2015; Strauss et al., 2022).

Confocal Image analysis

Cellular growth and expression quantifications were conducted using MorphoGraphX. Stacks were processed as described previously (Le Gloanec et al., 2022). After digitally removing the trichomes when necessary, the organ surface was detected with the ‘Edge detect’ tool with a threshold of 6000-13000, followed by the ‘Edge detect angle’ (3000-6500). An initial 5 µm cube size mesh was then created and subdivided three times before projecting the membrane signal (2-5 µm).

Cell segmentation and parent attribution were performed manually. Verification of cell parenting was done using 'Check correspondence'. Lineages over multiple days were calculated as described previously and manually corrected when required (Kierzkowski et al., 2019). Stomata were identified manually based on their morphology and developmental trajectory (Le Gloanec et al., 2022).

Metrics such as area expansion, cell proliferation, growth anisotropy, lobeyness, and cell size were computed as described before (Barbier de Reuille et al., 2015; Sapala et al., 2018). Growth rates along proximodistal and mediolateral axes were determined using a custom Bezier grid, manually adjusted to follow the organ geometry at each time point closely. Proximodistal and mediolateral distances from the organ base were calculated using the 'Cell distance' plugin, employing the 'Euclidean' parameter.

All figures were assembled using Adobe Photoshop or Adobe Illustrator software.

ACKNOWLEDGMENTS

We thank Binghan Wang and Jerome Burkiewicz for their assistance with data analysis and Charlotte Kirchhelle, Etienne Léveillé-Bourret, Vishwadeep Mane, Jason Reed, and Sylvia R. Silveira for suggestions and critical reading of the manuscript.

AUTHOR CONTRIBUTIONS

C.L., A.-L.R.-K., and D.K. conceived the project and its components. C.L. and A.G.-F. designed and performed the experiments. C.L., A.G-F., and V.A. analyzed the data. C.L., E.B., and D.K. drafted the manuscript. A.G.-F., V.A., and A.-L.R.-K. revised the manuscript. A.-L.R.-K. and D.K. supervised and funded the project.

FUNDING

This work was supported by Discovery grants (RGPIN-2018-05762 and RGPIN-2018-04897) from the Natural Sciences and Engineering Research Council of Canada to Daniel Kierzkowski and Anne-Lise Routier-Kierzkowska respectively, as well as Fonds de Recherche du Québec Nature et Technologies Team Grant (2021-PR-282285) to Daniel Kierzkowski and Anne-Lise Routier-Kierzkowska.

DATA AVAILABILITY

The data used to extract growth and all scripts used to analyze data are available to download from the Open Science Framework repository (link to be provided).

AUTHOR NOTES

The author responsible for distribution of materials integral to the findings presented in this article in accordance with the policy described in the Instructions for Authors (https://academic.oup.com/plcell/pages/General-Instructions) is Daniel Kierzkowski (daniel.kierzkowski@umontreal.ca).

Conflict of interest statement. None declared.

REFERENCES

Abley, K., Sauret-Güeto, S., Marée, A.F.M., and Coen, E. (2016). Formation of polarity convergences underlying shoot outgrowths. Elife **5**: e18165. https://doi.org/10.7554/eLife.18165

Alvarez, J.P., Furumizu, C., Efroni, I., Eshed, Y., and Bowman, J.L. (2016). Active suppression of a leaf meristem orchestrates determinate leaf growth. Elife **5**: e15023. https://doi.org/10.7554/eLife.15023

Andres-Robin, A., Reymond, M.C., Dupire, A., Battu, V., Dubrulle, N., Mouille, G., Lefebvre, V., Pelloux, J., Boudaoud, A., Traas, J., Scutt, C.P., and Monéger,

F. (2018). Evidence for the regulation of gynoecium morphogenesis by ETTIN via cell wall dynamics. Plant Physiol. **178**: 1222–1232. https://doi.org/10.1104/pp.18.00745

Andriankaja, M., Dhondt, S., DeBodt, S., Vanhaeren, H., Coppens, F., DeMilde, L., Mühlenbock, P., Skirycz, A., Gonzalez, N., Beemster, G.T.S., and Inzé, D. (2012). Exit from proliferation during leaf development in Arabidopsis thaliana: a not-so-gradual process. Dev. Cell **22**: 64–78. https://doi.org/10.1016/j.devcel.2011.11.011

Baerenfaller, K., Massonnet, C., Hennig, L., Russenberger, D., Sulpice, R., Walsh, S., Stitt, M., Granier, C., and Gruissem, W. (2015). A long photoperiod relaxes energy management in Arabidopsis leaf six. Curr. Plant Biol. **2**: 34–45. https://doi.org/10.1016/j.cpb.2015.07.001

Bar, M. and Ori, N. (2014). Leaf development and morphogenesis. Development **141**: 4219–4230. https://doi.org/10.1242/dev.106195

Barbier de Reuille, P. et al. (2015). MorphoGraphX: A platform for quantifying morphogenesis in 4D. Elife **4**: 05864. https://doi.org/10.7554/eLife.05864

Barkoulas, M., Hay, A., Kougioumoutzi, E., and Tsiantis, M. (2008). A developmental framework for dissected leaf formation in the Arabidopsis relative Cardamine hirsuta. Nat. Genet. **40**: 1136–1141. https://doi.org/10.1038/ng.189

Barth, S., Geier, T., Eimert, K., Watillon, B., Sangwan, R.S., and Gleissberg, S. (2009). KNOX overexpression in transgenic Kohleria (Gesneriaceae) prolongs the activity of proximal leaf blastozones and drastically alters segment fate. Planta **230**: 1081–1091. https://doi.org/10.1007/s00425-009-0997-0

Belteton, S.A., Sawchuk, M.G., Donohoe, B.S., Scarpella, E., and Szymanski, D.B. (2018). Reassessing the roles of PIN proteins and anticlinal microtubules during pavement cell morphogenesis. Plant Physiol. **176**: 432–449. https://doi.org/10.1104/pp.17.01554

Ben-Gera, H., Dafna, A., Alvarez, J.P., Bar, M., Mauerer, M., and Ori, N. (2016). Auxin-mediated lamina growth in tomato leaves is restricted by two parallel

717 mechanisms. Plant J. **86**: 443–457. https://doi.org/10.1111/tpj.13188

718 **Benková, E., Michniewicz, M., Sauer, M., Teichmann, T., Seifertová, D.,**
719 **Jürgens, G., and Friml, J.** (2003). Local, efflux-dependent auxin gradients as a
720 common module for plant organ formation. Cell **115**: 591–602.
721 https://doi.org/10.1016/S0092-8674(03)00924-3

722 **Berhin, A., Nawrath, C., and Hachez, C.** (2021). Subtle interplay between trichome
723 development and cuticle formation in plants. New Phytol. **233**: 2036–2046.
724 https://doi.org/10.1111/nph.17827

725 **Bielczynski, L.W., Łaçki, M.K., Hoefnagels, I., Gambin, A., and Croce, R.** (2017).
726 Leaf and plant age affects photosynthetic performance and photoprotective capacity.
727 Plant Physiol. **175**: 1634–1648. https://doi.org/10.1104/PP.17.00904

728 **Bilsborough, G.D., Runions, A., Barkoulas, M., Jenkins, H.W., Hasson, A.,**
729 **Galinha, C., Laufs, P., Hay, A., Prusinkiewicz, P., and Tsiantis, M.** (2011). Model
730 for the regulation of Arabidopsis thaliana leaf margin development. Proc. Natl. Acad.
731 Sci. U. S. A. **108**: 3424–3429. https://doi.org/10.1073/pnas.1015162108

732 **Bowman, J.L., Smyth, D.R., and Meyerowitz, E.M.** (1991). Genetic interactions
733 among floral homeotic genes of Arabidopsis. Development **112**: 1–20.
734 https://doi.org/10.1242/dev.112.1.1

735 **Bredmose, N. and Costes, E.** (2017). Axillary bud growth. In Reference Module in
736 Life Sciences (Elsevier). https://doi.org/10.1016/B978-0-12-809633-8.05056-1

737 **Burian, A., Paszkiewicz, G., Nguyen, K.T., Meda, S., Raczyńska-Szajgin, M., and**
738 **Timmermans, M.C.P.** (2022). Specification of leaf dorsiventrality via a prepatterned
739 binary readout of a uniform auxin input. Nat. Plants **8**: 269–280.
740 https://doi.org/10.1038/s41477-022-01111-3

741 **Burko, Y. and Ori, N.** (2013). The tomato leaf as a model system for organogenesis.
742 In Methods in Molecular Biology (Humana Press Inc.), pp. 1–19.
743 https://doi.org/10.1007/978-1-62703-221-6_1

744 **Cecchetti, V., Altamura, M.M., Brunetti, P., Petrocelli, V., Falasca, G., Ljung, K.,**

745 **Costantino, P., and Cardarelli, M.** (2013). Auxin controls Arabidopsis anther
746 dehiscence by regulating endothecium lignification and jasmonic acid biosynthesis.
747 Plant J. **74**: 411–422. https://doi.org/10.1111/tpj.12130

748 **Challa, K.R., Rath, M., and Nath, U.** (2019). The CIN-TCP transcription factors
749 promote commitment to differentiation in Arabidopsis leaf pavement cells via both
750 auxin-dependent and independent pathways. PLOS Genet. **15**: e1007988.
751 https://doi.org/10.1371/journal.pgen.1007988

752 **Challa, K.R., Rath, M., Sharma, A.N., Bajpai, A.K., Davuluri, S., Acharya, K.K.,**
753 **and Nath, U.** (2021). Active suppression of leaflet emergence as a mechanism of
754 simple leaf development. Nat. Plants **7**: 1264–1275. https://doi.org/10.1038/s41477-
755 021-00965-3

756 **Cooke, J.E.K., Eriksson, M.E., and Junttila, O.** (2012). The dynamic nature of bud
757 dormancy in trees: environmental control and molecular mechanisms. Plant. Cell
758 Environ. **35**: 1707–1728. https://doi.org/10.1111/j.1365-3040.2012.02552.x

759 **Cookson, S.J. and Granier, C.** (2006). A dynamic analysis of the shade-induced
760 plasticity in Arabidopsis thaliana rosette leaf development reveals new components
761 of the shade-adaptative response. Ann. Bot. **97**: 443–452.
762 https://doi.org/10.1093/aob/mcj047

763 **Ding, M., Zhu, Y., and Kinoshita, T.** (2023). Stomatal properties of Arabidopsis
764 cauline and rice flag leaves and their contributions to seed production and grain
765 yield. J. Exp. Bot. **74**: 1957–1973. https://doi.org/10.1093/jxb/erac492

766 **Ding, Z. and Friml, J.** (2010). Auxin regulates distal stem cell differentiation in
767 Arabidopsis roots. Proc. Natl. Acad. Sci. U. S. A. **107**: 12046–12051.
768 https://doi.org/10.1073/pnas.1000672107

769 **Donnelly, P.M., Bonetta, D., Tsukaya, H., Dengler, R.E., and Dengler, N.G.**
770 (1999). Cell cycling and cell enlargement in developing leaves of Arabidopsis. Dev.
771 Biol. **215**: 407–419. https://doi.org/10.1006/dbio.1999.9443

772 **Echevin, E., Le Gloanec, C., Skowrońska, N., Routier-Kierzkowska, A.-L.,**
773 **Burian, A., and Kierzkowski, D.** (2019). Growth and biomechanics of shoot organs.

774 J. Exp. Bot. **70**: 3573–3585. https://doi.org/10.1093/jxb/erz205

775 **Efroni, I., Eshed, Y., and Lifschitz, E.** (2010). Morphogenesis of simple and
776 compound leaves: a critical review. Plant Cell **22**: 1019–1032.
777 https://doi.org/10.1105/tpc.109.073601

778 **Fox, S. et al.** (2018). Spatiotemporal coordination of cell division and growth during
779 organ morphogenesis. PLoS Biol. **16**: e2005952.
780 https://doi.org/10.1371/journal.pbio.2005952

781 **Fukushima, K. and Hasebe, M.** (2014). Adaxial–abaxial polarity: the developmental
782 basis of leaf shape diversity. genesis **52**: 1–18. https://doi.org/10.1002/dvg.22728

783 **Le Gloanec, C., Collet, L., Silveira, S.R., Wang, B., Routier-Kierzkowska, A.L.,**
784 **and Kierzkowski, D.** (2022). Cell type-specific dynamics underlie cellular growth
785 variability in plants. Development **149**: dev200783.
786 https://doi.org/10.1242/dev.200783

787 **Gómez-Felipe, A., Marconi, M., Branchini, E., Wang, B., Bertrand-Rakusova, H.,**
788 **Stan, T., Burkiewicz, J., Folter, S. de, Routier-Kierzkowska, A.-L., Wabnik, K.,**
789 **and Kierzkowski, D.** (2023). Competing differentiation gradients coordinate fruit
790 morphogenesis. bioRxiv. https://doi.org/10.1101/2023.01.19.524793

791 **Green, A.A., Kennaway, J.R., Hanna, A.I., Bangham, J.A., and Coen, E.** (2010).
792 Genetic Control of Organ Shape and Tissue Polarity. PLoS Biol. **8**: e1000537.
793 https://doi.org/10.1371/journal.pbio.1000537

794 **Guenot, B., Bayer, E., Kierzkowski, D., Smith, R.S., Mandel, T., Zádníková, P.,**
795 **Benková, E., and Kuhlemeier, C.** (2012). PIN1-independent leaf initiation in
796 Arabidopsis. Plant Physiol. **159**: 1501–1510. https://doi.org/10.1104/pp.112.200402

797 **Hamant, O. and Saunders, T.E.** (2020). Shaping organs: shared structural
798 principles across kingdoms. Annu. Rev. Cell Dev. Biol. **36**: 385–410.
799 https://doi.org/10.1146/annurev-cellbio-012820-103850

800 **Hao, X., Tang, H., Wang, B., Wang, L., Cao, H., Wang, Y., Zeng, J., Fang, S.,**
801 **Chu, J., Yang, Y., and Wang, X.** (2019). Gene characterization and expression

802 analysis reveal the importance of auxin signaling in bud dormancy regulation in tea
803 plant. J. Plant Growth Regul. **38**: 225–240. https://doi.org/10.1007/s00344-018-
804 9834-7

805 **Harline, K. and Roeder, A.H.K.** (2023). An optimized pipeline for live imaging whole
806 Arabidopsis leaves at cellular resolution. Plant Methods **19**: 1–14.
807 https://doi.org/10.1186/s13007-023-00987-2

808 **Hay, A. and Tsiantis, M.** (2006). The genetic basis for differences in leaf form
809 between Arabidopsis thaliana and its wild relative Cardamine hirsuta. Nat. Genet. **38**:
810 942–947. https://doi.org/10.1038/ng1835

811 **He, J., Xu, M., Willmann, M.R., McCormick, K., Hu, T., Yang, L., Starker, C.G.,**
812 **Voytas, D.F., Meyers, B.C., and Poethig, R.S.** (2018). Threshold-dependent
813 repression of SPL gene expression by miR156/miR157 controls vegetative phase
814 change in Arabidopsis thaliana. PLOS Genet. **14**: e1007337.
815 https://doi.org/10.1371/journal.pgen.1007337

816 **He, Y., He, X., Wang, X., Hao, M., Gao, J., Wang, Y., Yang, Z.N., and Meng, X.**
817 (2023). An EPFL peptide signaling pathway promotes stamen elongation via
818 enhancing filament cell proliferation to ensure successful self-pollination in
819 Arabidopsis thaliana. New Phytol. **238**: 1045–1058.
820 https://doi.org/10.1111/nph.18806

821 **Heisler, M.G., Ohno, C., Das, P., Sieber, P., Reddy, G. V., Long, J.A., and**
822 **Meyerowitz, E.M.** (2005). Patterns of auxin transport and gene expression during
823 primordium development revealed by live imaging of the Arabidopsis inflorescence
824 meristem. Curr. Biol. **15**: 1899–1911. https://doi.org/10.1016/j.cub.2005.09.052

825 **Hempel, F.D. and Feldman, L.J.** (1994). Bi-directional inflorescence development in
826 Arabidopsis thaliana: Acropetal initiation of flowers and basipetal initiation of
827 paraclades. Planta **192**: 276–286. https://doi.org/10.1007/BF01089045

828 **Hervieux, N., Dumond, M., Sapala, A., Routier-Kierzkowska, A.-L., Kierzkowski,**
829 **D., Roeder, A.H.K., Smith, R.S., Boudaoud, A., and Hamant, O.** (2016). A
830 mechanical feedback restricts sepal growth and shape in Arabidopsis. Curr. Biol. **26**:

1019–1028. https://doi.org/10.1016/j.cub.2016.03.004

Honma, T. and Goto, K. (2001). Complexes of MADS-box proteins are sufficient to convert leaves into floral organs. Nature **409**: 525–529. https://doi.org/10.1038/35054083

Huang, H., Gong, Y., Liu, B., Wu, D., Zhang, M., Xie, D., and Song, S. (2020). The della proteins interact with MYB21 and MYB24 to regulate filament elongation in Arabidopsis. BMC Plant Biol. **20**: 1–9. https://doi.org/10.1186/s12870-020-2274-0

Huijser, P. and Schmid, M. (2011). The control of developmental phase transitions in plants. Development **138**: 4117–4129. https://doi.org/10.1242/dev.063511

Jaeger, J., Irons, D., and Monk, N. (2008). Regulative feedback in pattern formation: towards a general relativistic theory of positional information. Development **135**: 3175–3183. https://doi.org/10.1242/dev.018697

Jiao, Y., Du, F., and Traas, J. (2021). The mechanical feedback theory of leaf lamina formation. Trends Plant Sci. **26**: 107–110. https://doi.org/10.1016/j.tplants.2020.11.005

Junttila, O. and Hänninen, H. (2012). The minimum temperature for budburst in Betula depends on the state of dormancy. Tree Physiol. **32**: 337–345. https://doi.org/10.1093/treephys/tps010

Karabourniotis, G., Liakopoulos, G., Nikolopoulos, D., and Bresta, P. (2020). Protective and defensive roles of non-glandular trichomes against multiple stresses: structure–function coordination. J. For. Res. **31**: 1–12. https://doi.org/10.1007/s11676-019-01034-4

Kasprzewska, A., Carter, R., Swarup, R., Bennett, M., Monk, N., Hobbs, J.K., and Fleming, A. (2015). Auxin influx importers modulate serration along the leaf margin. Plant J. **83**: 705–718. https://doi.org/10.1111/tpj.12921

Kierzkowski, D. et al. (2019). A growth-based framework for leaf shape development and diversity. Cell **177**: 1405–1418. https://doi.org/10.1016/j.cell.2019.05.011

Krizek, B.A. and Meyerowitz, E.M. (1996). The Arabidopsis homeotic genes APETALA3 and PISTILLATA are sufficient to provide the B class organ identity function. Development **122**: 11–22. https://doi.org/10.1242/dev.122.1.11

Kuchen, E.E., Fox, S., de Reuille, P.B., Kennaway, R., Bensmihen, S., Avondo, J., Calder, G.M., Southam, P., Robinson, S., Bangham, A., and Coen, E. (2012). Generation of leaf shape through early patterns of growth and tissue polarity. Science **335**: 1092–1096. https://doi.org/10.1126/science.1214678

Lampugnani, E.R., Kilinc, A., and Smyth, D.R. (2013). Auxin controls petal initiation in Arabidopsis. Development **140**: 185–194. https://doi.org/10.1242/dev.084582

Liao, C.Y., Smet, W., Brunoud, G., Yoshida, S., Vernoux, T., and Weijers, D. (2015). Reporters for sensitive and quantitative measurement of auxin response. Nat. Methods **12**: 207–210. https://doi.org/10.1038/nmeth.3279

Liu, T., Longhurst, A.D., Talavera-Rauh, F., Hokin, S.A., and Barton, M.K. (2016). The arabidopsis transcription factor ABIG1 relays ABA signaled growth inhibition and drought induced senescence. Elife **5**: e13768. https://doi.org/10.7554/eLife.13768

Di Mambro, R. et al. (2017). Auxin minimum triggers the developmental switch from cell division to cell differentiation in the Arabidopsis root. Proc. Natl. Acad. Sci. U. S. A. **114**: E7641–E7649. https://doi.org/10.1073/pnas.1705833114

Mansfield, C., Newman, J.L., Olsson, T.S.G., Hartley, M., Chan, J., and Coen, E. (2018). Ectopic BASL reveals tissue cell polarity throughout leaf development in Arabidopsis thaliana. Curr. Biol. **28**: 2638–2646. https://doi.org/10.1016/j.cub.2018.06.019

Martignago, D., Siemiatkowska, B., Lombardi, A., and Conti, L. (2020). Abscisic acid and flowering regulation: many targets, different places. Int. J. Mol. Sci. **21**: 9700. https://doi.org/10.3390/ijms21249700

Massonnet, C. et al. (2010). Probing the reproducibility of leaf growth and molecular phenotypes: a comparison of three Arabidopsis accessions cultivated in ten

laboratories. Plant Physiol. **152**: 2142–2157. https://doi.org/10.1104/pp.109.148338

Maugarny-Calès, A. and Laufs, P. (2018). Getting leaves into shape: A molecular, cellular, environmental and evolutionary view. Development **145**: dev161646. https://doi.org/10.1242/dev.161646

Melnyk, C.W., Schuster, C., Leyser, O., and Meyerowitz, E.M. (2015). A developmental framework for graft formation and vascular reconnection in Arabidopsis thaliana. Curr. Biol. **25**: 1306–1318. https://doi.org/10.1016/j.cub.2015.03.032

Nagpal, P., Ellis, C.M., Weber, H., Ploense, S.E., Barkawi, L.S., Guilfoyle, T.J., Hagen, G., Alonso, J.M., Cohen, J.D., Farmer, E.E., Ecker, J.R., and Reed, J.W. (2005). Auxin response factors ARF6 and ARF8 promote jasmonic acid production and flower maturation. Development **132**: 4107–4118. https://doi.org/10.1242/dev.01955

Nakayama, H., Nakayama, N., Seiki, S., Kojima, M., Sakakibara, H., Sinha, N., and Kimuraa, S. (2014). Regulation of the KNOX-GA gene module induces heterophyllic alteration in North American lake cress. Plant Cell **26**: 4733–4748. https://doi.org/10.1105/tpc.114.130229

Nikovics, K., Blein, T., Peaucelle, A., Ishida, T., Morin, H., Aida, M., and Laufs, P. (2006). The balance between the MIR164A and CUC2 genes controls leaf margin serration in Arabidopsis. Plant Cell **18**: 2929–2945. https://doi.org/10.1105/tpc.106.045617

Ori, N. et al. (2007). Regulation of LANCEOLATE by miR319 is required for compound-leaf development in tomato. Nat. Genet. **39**: 787–791. https://doi.org/10.1038/ng2036

Pabõn-Mora, N., Sharma, B., Holappa, L.D., Kramer, E.M., and Litt, A. (2013). The Aquilegia FRUITFULL-like genes play key roles in leaf morphogenesis and inflorescence development. Plant J. **74**: 197–212. https://doi.org/10.1111/tpj.12113

Pastore, J.J., Limpuangthip, A., Yamaguchi, N., Wu, M.F., Sang, Y., Han, S.K., Malaspina, L., Chavdaroff, N., Yamaguchi, A., and Wagner, D. (2011). LATE

MERISTEM IDENTITY2 acts together with LEAFY to activate APETALA1. Development **138**: 3189–3198. https://doi.org/10.1242/dev.063073

Pelaz, S., Tapia-López, R., Alvarez-Buylla, E.R., and Yanofsky, M.F. (2001). Conversion of leaves into petals in Arabidopsis. Curr. Biol. **11**: 182–184. https://doi.org/10.1016/S0960-9822(01)00024-0

Reeves, P.H. et al. (2012). A regulatory network for coordinated flower maturation. PLOS Genet. **8**: e1002506. https://doi.org/10.1371/journal.pgen.1002506

Rinne, P.L.H., Welling, A., Vahala, J., Ripel, L., Ruonala, R., Kangasjärvi, J., and van der Schoot, C. (2011). Chilling of dormant buds hyperinduces FLOWERING LOCUS T and recruits GA-inducible 1,3-β-glucanases to reopen signal conduits and release dormancy in Populus. Plant Cell **23**: 130–146. https://doi.org/10.1105/tpc.110.081307

Rodriguez, R.E., Debernardi, J.M., and Palatnik, J.F. (2014). Morphogenesis of simple leaves: regulation of leaf size and shape. Wiley Interdiscip. Rev. Dev. Biol. **3**: 41–57. https://doi.org/10.1002/wdev.115

Roeder, A.H.K., Chickarmane, V., Cunha, A., Obara, B., Manjunath, B.S., and Meyerowitz, E.M. (2010). Variability in the control of cell division underlies sepal epidermal patterning in Arabidopsis thaliana. PLoS Biol. **8**: e1000367. https://doi.org/10.1371/journal.pbio.1000367

Runions, A., Tsiantis, M., and Prusinkiewicz, P. (2017). A common developmental program can produce diverse leaf shapes. New Phytol. **216**: 401–418. https://doi.org/10.1111/nph.14449

Sablowski, R. (2015). Control of patterning, growth, and differentiation by floral organ identity genes. J. Exp. Bot. **66**: 1065–1073. https://doi.org/10.1093/jxb/eru514

Salem, M.A., Li, Y., Bajdzienko, K., Fisahn, J., Watanabe, M., Hoefgen, R., Schöttler, M.A., and Giavalisco, P. (2018). RAPTOR controls developmental growth transitions by altering the hormonal and metabolic balance. Plant Physiol. **177**: 565–593. https://doi.org/10.1104/pp.17.01711

Sapala, A. et al. (2018). Why plants make puzzle cells, and how their shape emerges. Elife **7**: e32794. https://doi.org/10.7554/eLife.32794

Sauret-Güeto, S., Schiessl, K., Bangham, A., Sablowski, R., and Coen, E. (2013). JAGGED controls arabidopsis petal growth and shape by interacting with a divergent polarity field. PLoS Biol. **11**: e1001550. https://doi.org/10.1371/journal.pbio.1001550

Schiessl, K., Kausika, S., Southam, P., Bush, M., and Sablowski, R. (2012). JAGGED controls growth anisotropy and coordination between cell size and cell cycle during plant organogenesis. Curr. Biol. **22**: 1739–1746. https://doi.org/10.1016/j.cub.2012.07.020

Schwarz, S., Grande, A. V., Bujdoso, N., Saedler, H., and Huijser, P. (2008). The microRNA regulated SBP-box genes SPL9 and SPL15 control shoot maturation in Arabidopsis. Plant Mol. Biol. **67**: 183–195. https://doi.org/10.1007/s11103-008-9310-z

Shani, E., Ben-Gera, H., Shleizer-Burko, S., Burko, Y., Weiss, D., and Ori, N. (2010). Cytokinin regulates compound leaf development in tomato. Plant Cell **22**: 3206–3217. https://doi.org/10.1105/tpc.110.078253

Shikata, M., Koyama, T., Mitsuda, N., and Ohme-Takagi, M. (2009). Arabidopsis SBP-Box genes SPL10, SPL11 and SPL2 control morphological change in association with shoot maturation in the reproductive phase. Plant Cell Physiol. **50**: 2133–2145. https://doi.org/10.1093/pcp/pcp148

Silveira, S.R., Le Gloanec, C., Gómez-Felipe, A., Routier-Kierzkowska, A.-L.L., and Kierzkowski, D. (2022). Live-imaging provides an atlas of cellular growth dynamics in the stamen. Plant Physiol. **188**: 769–781. https://doi.org/10.1093/plphys/kiab363

Smyth, D.R., Bowman, J.L., and Meyerowitz, E.M. (1990). Early flower development in Arabidopsis. Plant Cell **2**: 755–767. https://doi.org/10.1105/tpc.2.8.755

Strauss, S. et al. (2022). Using positional information to provide context for

biological image analysis with MorphoGraphX 2.0. Elife **11**: e72601. https://doi.org/10.7554/eLife.72601

Su, H., Abernathy, S.D., White, R.H., and Finlayson, S.A. (2011). Photosynthetic photon flux density and phytochrome B interact to regulate branching in Arabidopsis. Plant. Cell Environ. **34**: 1986–1998. https://doi.org/10.1111/j.1365-3040.2011.02393.x

Tang, H.-B., Wang, J., Wang, L., Shang, G.-D., Xu, Z.-G., Mai, Y.-X., Liu, Y.-T., Zhang, T.-Q., and Wang, J.-W. (2023). Anisotropic cell growth at the leaf base promotes age-related changes in leaf shape in Arabidopsis thaliana. Plant Cell **35**: 1386–1407. https://doi.org/10.1093/plcell/koad031

Vlad, D. et al. (2014). Leaf shape evolution through duplication, regulatory diversification and loss of a homeobox gene. Science **343**: 780–783. https://doi.org/10.1126/science.1248384

Vuolo, F. et al. (2018). LMI1 homeodomain protein regulates organ proportions by spatial modulation of endoreduplication. Genes Dev. **32**: 1361–1366. https://doi.org/10.1101/gad.318212.118

Wang, Y., Strauss, S., Liu, S., Pieper, B., Lymbouridou, R., Runions, A., and Tsiantis Correspondence, M. (2022). The cellular basis for synergy between RCO and KNOX1 homeobox genes in leaf shape diversity. Curr. Biol. **32**: 3773-3784.e5. https://doi.org/10.1016/j.cub.2022.08.020

Werner, S., Bartrina, I., Novák, O., Strnad, M., Werner, T., and Schmülling, T. (2021). The cytokinin status of the epidermis regulates aspects of vegetative and reproductive development in Arabidopsis thaliana. Front. Plant Sci. **12**: 613488. https://doi.org/10.3389/fpls.2021.613488

Whitewoods, C.D., Gonçalves, B., Cheng, J., Cui, M., Kennaway, R., Lee, K., Bushell, C., Yu, M., Piao, C., and Coen, E. (2020). Evolution of carnivorous traps from planar leaves through simple shifts in gene expression. Science **367**: 91–96. https://doi.org/10.1126/science.aay5433

Willis, L., Refahi, Y., Wightman, R., Landrein, B., Teles, J., Huang, K.C.,

Meyerowitz, E.M., and Jönsson, H. (2016). Cell size and growth regulation in the Arabidopsis thaliana apical stem cell niche. Proc. Natl. Acad. Sci. U. S. A. **113**: E8238–E8246. https://doi.org/10.1073/pnas.1616768113

Wu, W., Du, K., Kang, X., and Wei, H. (2021). The diverse roles of cytokinins in regulating leaf development. Hortic. Res. **8**: 118. https://doi.org/10.1038/s41438-021-00558-3

Xu, M., Hu, T., Zhao, J., Park, M.Y., Earley, K.W., Wu, G., Yang, L., and Poethig, R.S. (2016). Developmental functions of miR156-regulated SQUAMOSA PROMOTER BINDING PROTEIN-LIKE (SPL) genes in Arabidopsis thaliana. PLOS Genet. **12**: e1006263. https://doi.org/10.1371/journal.pgen.1006263

Yadav, A.S., Hong, L., Klees, P.M., Kiss, A., He, X., Barrios, I.M., Heeney, M., Galang, A.M.D., Smith, R.S., Boudaoud, A., and Roeder, A.H.K. (2023). Growth directions and stiffness across cell layers determine whether tissues stay smooth or buckle. bioRxiv. https://doi.org/10.1101/2023.07.22.549953

Yang, M. and Jiao, Y. (2016). Regulation of axillary meristem initiation by transcription factors and plant hormones. Front. Plant Sci. **7**. https://doi.org/10.3389/fpls.2016.00183

Yu, S., Lian, H., and Wang, J.W. (2015). Plant developmental transitions: the role of microRNAs and sugars. Curr. Opin. Plant Biol. **27**: 1–7. https://doi.org/10.1016/j.pbi.2015.05.009

Žádníkova, P. et al. (2010). Role of PIN-mediated auxin efflux in apical hook development of Arabidopsis thaliana. Development **137**: 607–617. https://doi.org/10.1242/dev.041277

Zhang, Z., Runions, A., Mentink, R.A., Kierzkowski, D., Karady, M., Hashemi, B., Huijser, P., Strauss, S., Gan, X., Ljung, K., and Tsiantis, M. (2020). A WOX/auxin biosynthesis module controls growth to shape leaf form. Curr. Biol. **30**: 4857-4868.e6. https://doi.org/10.1016/j.cub.2020.09.037

Zhao, F. et al. (2020). Microtubule-mediated wall anisotropy contributes to leaf blade flattening. Curr. Biol. **30**: 3972-3985.e6. https://doi.org/10.1016/j.cub.2020.07.076

1032

Parsed Citations

Abley, K., Sauret-Güeto, S., Marée, A.F.M., and Coen, E. (2016). Formation of polarity convergences underlying shoot outgrowths. Elife 5: e18165. https://doi.org/10.7554/eLife.18165
Google Scholar: Author Only Title Only Author and Title

Alvarez, J.P., Furumizu, C., Efroni, I., Eshed, Y., and Bowman, J.L. (2016). Active suppression of a leaf meristem orchestrates determinate leaf growth. Elife 5: e15023. https://doi.org/10.7554/eLife.15023
Google Scholar: Author Only Title Only Author and Title

Andres-Robin, A., Reymond, M.C., Dupire, A., Battu, V., Dubrulle, N., Mouille, G., Lefebvre, V., Pelloux, J., Boudaoud, A., Traas, J., Scutt, C.P., and Monéger, F. (2018). Evidence for the regulation of gynoecium morphogenesis by ETTIN via cell wall dynamics. Plant Physiol. 178: 1222–1232. https://doi.org/10.1104/pp.18.00745
Google Scholar: Author Only Title Only Author and Title

Andriankaja, M., Dhondt, S., DeBodt, S., Vanhaeren, H., Coppens, F., DeMilde, L., Mühlenbock, P., Skirycz, A., Gonzalez, N., Beemster, G.T.S., and Inzé, D. (2012). Exit from proliferation during leaf development in Arabidopsis thaliana: a not-so-gradual process. Dev. Cell 22: 64–78. https://doi.org/10.1016/j.devcel.2011.11.011
Google Scholar: Author Only Title Only Author and Title

Baerenfaller, K., Massonnet, C., Hennig, L., Russenberger, D., Sulpice, R., Walsh, S., Stitt, M., Granier, C., and Gruissem, W. (2015). A long photoperiod relaxes energy management in Arabidopsis leaf six. Curr. Plant Biol. 2: 34–45. https://doi.org/10.1016/j.cpb.2015.07.001
Google Scholar: Author Only Title Only Author and Title

Bar, M. and Ori, N. (2014). Leaf development and morphogenesis. Development 141: 4219–4230. https://doi.org/10.1242/dev.106195
Google Scholar: Author Only Title Only Author and Title

Barbier de Reuille, P. et al. (2015). MorphoGraphX: A platform for quantifying morphogenesis in 4D. Elife 4: 05864. https://doi.org/10.7554/eLife.05864
Google Scholar: Author Only Title Only Author and Title

Barkoulas, M., Hay, A., Kougioumoutzi, E., and Tsiantis, M. (2008). A developmental framework for dissected leaf formation in the Arabidopsis relative Cardamine hirsuta. Nat. Genet. 40: 1136–1141. https://doi.org/10.1038/ng.189
Google Scholar: Author Only Title Only Author and Title

Barth, S., Geier, T., Eimert, K., Watillon, B., Sangwan, R.S., and Gleissberg, S. (2009). KNOX overexpression in transgenic Kohleria (Gesneriaceae) prolongs the activity of proximal leaf blastozones and drastically alters segment fate. Planta 230: 1081–1091. https://doi.org/10.1007/s00425-009-0997-0
Google Scholar: Author Only Title Only Author and Title

Belteton, S.A., Sawchuk, M.G., Donohoe, B.S., Scarpella, E., and Szymanski, D.B. (2018). Reassessing the roles of PIN proteins and anticlinal microtubules during pavement cell morphogenesis. Plant Physiol. 176: 432–449. https://doi.org/10.1104/pp.17.01554
Google Scholar: Author Only Title Only Author and Title

Ben-Gera, H., Dafna, A., Alvarez, J.P., Bar, M., Mauerer, M., and Ori, N. (2016). Auxin-mediated lamina growth in tomato leaves is restricted by two parallel mechanisms. Plant J. 86: 443–457. https://doi.org/10.1111/tpj.13188
Google Scholar: Author Only Title Only Author and Title

Benková, E., Michniewicz, M., Sauer, M., Teichmann, T., Seifertová, D., Jürgens, G., and Friml, J. (2003). Local, efflux-dependent auxin gradients as a common module for plant organ formation. Cell 115: 591–602. https://doi.org/10.1016/S0092-8674(03)00924-3
Google Scholar: Author Only Title Only Author and Title

Berhin, A., Nawrath, C., and Hachez, C. (2021). Subtle interplay between trichome development and cuticle formation in plants. New Phytol. 233: 2036–2046. https://doi.org/10.1111/nph.17827
Google Scholar: Author Only Title Only Author and Title

Bielczynski, L.W., Łaçki, M.K., Hoefnagels, I., Gambin, A., and Croce, R. (2017). Leaf and plant age affects photosynthetic performance and photoprotective capacity. Plant Physiol. 175: 1634–1648. https://doi.org/10.1104/PP.17.00904
Google Scholar: Author Only Title Only Author and Title

Bilsborough, G.D., Runions, A., Barkoulas, M., Jenkins, H.W., Hasson, A., Galinha, C., Laufs, P., Hay, A., Prusinkiewicz, P., and Tsiantis, M. (2011). Model for the regulation of Arabidopsis thaliana leaf margin development. Proc. Natl. Acad. Sci. U. S. A. 108: 3424–3429. https://doi.org/10.1073/pnas.1015162108
Google Scholar: Author Only Title Only Author and Title

Bowman, J.L., Smyth, D.R., and Meyerowitz, E.M. (1991). Genetic interactions among floral homeotic genes of Arabidopsis. Development 112: 1–20. https://doi.org/10.1242/dev.112.1.1
Google Scholar: Author Only Title Only Author and Title

Bredmose, N. and Costes, E. (2017). Axillary bud growth. In Reference Module in Life Sciences (Elsevier). https://doi.org/10.1016/B978-0-12-809633-8.05056-1
Google Scholar: Author Only Title Only Author and Title

Burian, A., Paszkiewicz, G., Nguyen, K.T., Meda, S., Raczyńska-Szajgin, M., and Timmermans, M.C.P. (2022). Specification of leaf dorsiventrality via a prepatterned binary readout of a uniform auxin input. Nat. Plants 8: 269–280. https://doi.org/10.1038/s41477-022-01111-3
Google Scholar: Author Only Title Only Author and Title

Burko, Y. and Ori, N. (2013). The tomato leaf as a model system for organogenesis. In Methods in Molecular Biology (Humana Press Inc.), pp. 1–19. https://doi.org/10.1007/978-1-62703-221-6_1
Google Scholar: Author Only Title Only Author and Title

Cecchetti, V., Altamura, M.M., Brunetti, P., Petrocelli, V., Falasca, G., Ljung, K., Costantino, P., and Cardarelli, M. (2013). Auxin controls Arabidopsis anther dehiscence by regulating endothecium lignification and jasmonic acid biosynthesis. Plant J. 74: 411–422. https://doi.org/10.1111/tpj.12130
Google Scholar: Author Only Title Only Author and Title

Challa, K.R., Rath, M., and Nath, U. (2019). The CIN-TCP transcription factors promote commitment to differentiation in Arabidopsis leaf pavement cells via both auxin-dependent and independent pathways. PLOS Genet. 15: e1007988. https://doi.org/10.1371/journal.pgen.1007988
Google Scholar: Author Only Title Only Author and Title

Challa, K.R., Rath, M., Sharma, A.N., Bajpai, A.K., Davuluri, S., Acharya, K.K., and Nath, U. (2021). Active suppression of leaflet emergence as a mechanism of simple leaf development. Nat. Plants 7: 1264–1275. https://doi.org/10.1038/s41477-021-00965-3
Google Scholar: Author Only Title Only Author and Title

Cooke, J.E.K., Eriksson, M.E., and Junttila, O. (2012). The dynamic nature of bud dormancy in trees: environmental control and molecular mechanisms. Plant. Cell Environ. 35: 1707–1728. https://doi.org/10.1111/j.1365-3040.2012.02552.x
Google Scholar: Author Only Title Only Author and Title

Cookson, S.J. and Granier, C. (2006). A dynamic analysis of the shade-induced plasticity in Arabidopsis thaliana rosette leaf development reveals new components of the shade-adaptative response. Ann. Bot. 97: 443–452. https://doi.org/10.1093/aob/mcj047
Google Scholar: Author Only Title Only Author and Title

Ding, M., Zhu, Y., and Kinoshita, T. (2023). Stomatal properties of Arabidopsis cauline and rice flag leaves and their contributions to seed production and grain yield. J. Exp. Bot. 74: 1957–1973. https://doi.org/10.1093/jxb/erac492
Google Scholar: Author Only Title Only Author and Title

Ding, Z. and Friml, J. (2010). Auxin regulates distal stem cell differentiation in Arabidopsis roots. Proc. Natl. Acad. Sci. U. S. A. 107: 12046–12051. https://doi.org/10.1073/pnas.1000672107
Google Scholar: Author Only Title Only Author and Title

Donnelly, P.M., Bonetta, D., Tsukaya, H., Dengler, R.E., and Dengler, N.G. (1999). Cell cycling and cell enlargement in developing leaves of Arabidopsis. Dev. Biol. 215: 407–419. https://doi.org/10.1006/dbio.1999.9443
Google Scholar: Author Only Title Only Author and Title

Echevin, E., Le Gloanec, C., Skowrońska, N., Routier-Kierzkowska, A.-L., Burian, A., and Kierzkowski, D. (2019). Growth and biomechanics of shoot organs. J. Exp. Bot. 70: 3573–3585. https://doi.org/10.1093/jxb/erz205
Google Scholar: Author Only Title Only Author and Title

Efroni, I., Eshed, Y., and Lifschitz, E. (2010). Morphogenesis of simple and compound leaves: a critical review. Plant Cell 22: 1019–1032. https://doi.org/10.1105/tpc.109.073601
Google Scholar: Author Only Title Only Author and Title

Fox, S. et al. (2018). Spatiotemporal coordination of cell division and growth during organ morphogenesis. PLoS Biol. 16: e2005952. https://doi.org/10.1371/journal.pbio.2005952
Google Scholar: Author Only Title Only Author and Title

Fukushima, K. and Hasebe, M. (2014). Adaxial–abaxial polarity: the developmental basis of leaf shape diversity. genesis 52: 1–18. https://doi.org/10.1002/dvg.22728
Google Scholar: Author Only Title Only Author and Title

Le Gloanec, C., Collet, L., Silveira, S.R., Wang, B., Routier-Kierzkowska, A.L., and Kierzkowski, D. (2022). Cell type-specific dynamics underlie cellular growth variability in plants. Development 149: dev200783. https://doi.org/10.1242/dev.200783
Google Scholar: Author Only Title Only Author and Title

Gómez-Felipe, A., Marconi, M., Branchini, E., Wang, B., Bertrand-Rakusova, H., Stan, T., Burkiewicz, J., Folter, S. de, Routier-Kierzkowska, A.-L., Wabnik, K., and Kierzkowski, D. (2023). Competing differentiation gradients coordinate fruit morphogenesis.

bioRxiv. https://doi.org/10.1101/2023.01.19.524793
Google Scholar: Author Only Title Only Author and Title

Green, A.A., Kennaway, J.R., Hanna, A.I., Bangham, J.A., and Coen, E. (2010). Genetic Control of Organ Shape and Tissue Polarity. PLoS Biol. 8: e1000537. https://doi.org/10.1371/journal.pbio.1000537
Google Scholar: Author Only Title Only Author and Title

Guenot, B., Bayer, E., Kierzkowski, D., Smith, R.S., Mandel, T., Zádníková, P., Benková, E., and Kuhlemeier, C. (2012). PIN1-independent leaf initiation in Arabidopsis. Plant Physiol. 159: 1501–1510. https://doi.org/10.1104/pp.112.200402
Google Scholar: Author Only Title Only Author and Title

Hamant, O. and Saunders, T.E. (2020). Shaping organs: shared structural principles across kingdoms. Annu. Rev. Cell Dev. Biol. 36: 385–410. https://doi.org/10.1146/annurev-cellbio-012820-103850
Google Scholar: Author Only Title Only Author and Title

Hao, X., Tang, H., Wang, B., Wang, L., Cao, H., Wang, Y., Zeng, J., Fang, S., Chu, J., Yang, Y., and Wang, X. (2019). Gene characterization and expression analysis reveal the importance of auxin signaling in bud dormancy regulation in tea plant. J. Plant Growth Regul. 38: 225–240. https://doi.org/10.1007/s00344-018-9834-7
Google Scholar: Author Only Title Only Author and Title

Harline, K. and Roeder, A.H.K. (2023). An optimized pipeline for live imaging whole Arabidopsis leaves at cellular resolution. Plant Methods 19: 1–14. https://doi.org/10.1186/s13007-023-00987-2
Google Scholar: Author Only Title Only Author and Title

Hay, A. and Tsiantis, M. (2006). The genetic basis for differences in leaf form between Arabidopsis thaliana and its wild relative Cardamine hirsuta. Nat. Genet. 38: 942–947. https://doi.org/10.1038/ng1835
Google Scholar: Author Only Title Only Author and Title

He, J., Xu, M., Willmann, M.R., McCormick, K., Hu, T., Yang, L., Starker, C.G., Voytas, D.F., Meyers, B.C., and Poethig, R.S. (2018). Threshold-dependent repression of SPL gene expression by miR156/miR157 controls vegetative phase change in Arabidopsis thaliana. PLOS Genet. 14: e1007337. https://doi.org/10.1371/journal.pgen.1007337
Google Scholar: Author Only Title Only Author and Title

He, Y., He, X., Wang, X., Hao, M., Gao, J., Wang, Y., Yang, Z.N., and Meng, X. (2023). An EPFL peptide signaling pathway promotes stamen elongation via enhancing filament cell proliferation to ensure successful self-pollination in Arabidopsis thaliana. New Phytol. 238: 1045–1058. https://doi.org/10.1111/nph.18806
Google Scholar: Author Only Title Only Author and Title

Heisler, M.G., Ohno, C., Das, P., Sieber, P., Reddy, G. V., Long, J.A., and Meyerowitz, E.M. (2005). Patterns of auxin transport and gene expression during primordium development revealed by live imaging of the Arabidopsis inflorescence meristem. Curr. Biol. 15: 1899–1911. https://doi.org/10.1016/j.cub.2005.09.052
Google Scholar: Author Only Title Only Author and Title

Hempel, F.D. and Feldman, L.J. (1994). Bi-directional inflorescence development in Arabidopsis thaliana: Acropetal initiation of flowers and basipetal initiation of paraclades. Planta 192: 276–286. https://doi.org/10.1007/BF01089045
Google Scholar: Author Only Title Only Author and Title

Hervieux, N., Dumond, M., Sapala, A., Routier-Kierzkowska, A.-L., Kierzkowski, D., Roeder, A.H.K., Smith, R.S., Boudaoud, A., and Hamant, O. (2016). A mechanical feedback restricts sepal growth and shape in Arabidopsis. Curr. Biol. 26: 1019–1028. https://doi.org/10.1016/j.cub.2016.03.004
Google Scholar: Author Only Title Only Author and Title

Honma, T. and Goto, K. (2001). Complexes of MADS-box proteins are sufficient to convert leaves into floral organs. Nature 409: 525–529. https://doi.org/10.1038/35054083
Google Scholar: Author Only Title Only Author and Title

Huang, H., Gong, Y., Liu, B., Wu, D., Zhang, M., Xie, D., and Song, S. (2020). The della proteins interact with MYB21 and MYB24 to regulate filament elongation in Arabidopsis. BMC Plant Biol. 20: 1–9. https://doi.org/10.1186/s12870-020-2274-0
Google Scholar: Author Only Title Only Author and Title

Huijser, P. and Schmid, M. (2011). The control of developmental phase transitions in plants. Development 138: 4117–4129. https://doi.org/10.1242/dev.063511
Google Scholar: Author Only Title Only Author and Title

Jaeger, J., Irons, D., and Monk, N. (2008). Regulative feedback in pattern formation: towards a general relativistic theory of positional information. Development 135: 3175–3183. https://doi.org/10.1242/dev.018697
Google Scholar: Author Only Title Only Author and Title

Jiao, Y., Du, F., and Traas, J. (2021). The mechanical feedback theory of leaf lamina formation. Trends Plant Sci. 26: 107–110. https://doi.org/10.1016/j.tplants.2020.11.005

Google Scholar: Author Only Title Only Author and Title

Junttila, O. and Hänninen, H. (2012). The minimum temperature for budburst in Betula depends on the state of dormancy. Tree Physiol. 32: 337–345. https://doi.org/10.1093/treephys/tps010
Google Scholar: Author Only Title Only Author and Title

Karabourniotis, G., Liakopoulos, G., Nikolopoulos, D., and Bresta, P. (2020). Protective and defensive roles of non-glandular trichomes against multiple stresses: structure–function coordination. J. For. Res. 31: 1–12. https://doi.org/10.1007/s11676-019-01034-4
Google Scholar: Author Only Title Only Author and Title

Kasprzewska, A., Carter, R., Swarup, R., Bennett, M., Monk, N., Hobbs, J.K., and Fleming, A. (2015). Auxin influx importers modulate serration along the leaf margin. Plant J. 83: 705–718. https://doi.org/10.1111/tpj.12921
Google Scholar: Author Only Title Only Author and Title

Kierzkowski, D. et al. (2019). A growth-based framework for leaf shape development and diversity. Cell 177: 1405–1418. https://doi.org/10.1016/j.cell.2019.05.011
Google Scholar: Author Only Title Only Author and Title

Krizek, B.A. and Meyerowitz, E.M. (1996). The Arabidopsis homeotic genes APETALA3 and PISTILLATA are sufficient to provide the B class organ identity function. Development 122: 11–22. https://doi.org/10.1242/dev.122.1.11
Google Scholar: Author Only Title Only Author and Title

Kuchen, E.E., Fox, S., de Reuille, P.B., Kennaway, R., Bensmihen, S., Avondo, J., Calder, G.M., Southam, P., Robinson, S., Bangham, A., and Coen, E. (2012). Generation of leaf shape through early patterns of growth and tissue polarity. Science 335: 1092–1096. https://doi.org/10.1126/science.1214678
Google Scholar: Author Only Title Only Author and Title

Lampugnani, E.R., Kilinc, A., and Smyth, D.R. (2013). Auxin controls petal initiation in Arabidopsis. Development 140: 185–194. https://doi.org/10.1242/dev.084582
Google Scholar: Author Only Title Only Author and Title

Liao, C.Y., Smet, W., Brunoud, G., Yoshida, S., Vernoux, T., and Weijers, D. (2015). Reporters for sensitive and quantitative measurement of auxin response. Nat. Methods 12: 207–210. https://doi.org/10.1038/nmeth.3279
Google Scholar: Author Only Title Only Author and Title

Liu, T., Longhurst, A.D., Talavera-Rauh, F., Hokin, S.A., and Barton, M.K. (2016). The arabidopsis transcription factor ABIG1 relays ABA signaled growth inhibition and drought induced senescence. Elife 5: e13768. https://doi.org/10.7554/eLife.13768
Google Scholar: Author Only Title Only Author and Title

Di Mambro, R. et al. (2017). Auxin minimum triggers the developmental switch from cell division to cell differentiation in the Arabidopsis root. Proc. Natl. Acad. Sci. U. S. A. 114: E7641–E7649. https://doi.org/10.1073/pnas.1705833114
Google Scholar: Author Only Title Only Author and Title

Mansfield, C., Newman, J.L., Olsson, T.S.G., Hartley, M., Chan, J., and Coen, E. (2018). Ectopic BASL reveals tissue cell polarity throughout leaf development in Arabidopsis thaliana. Curr. Biol. 28: 2638–2646. https://doi.org/10.1016/j.cub.2018.06.019
Google Scholar: Author Only Title Only Author and Title

Martignago, D., Siemiatkowska, B., Lombardi, A., and Conti, L. (2020). Abscisic acid and flowering regulation: many targets, different places. Int. J. Mol. Sci. 21: 9700. https://doi.org/10.3390/ijms21249700
Google Scholar: Author Only Title Only Author and Title

Massonnet, C. et al. (2010). Probing the reproducibility of leaf growth and molecular phenotypes: a comparison of three Arabidopsis accessions cultivated in ten laboratories. Plant Physiol. 152: 2142–2157. https://doi.org/10.1104/pp.109.148338
Google Scholar: Author Only Title Only Author and Title

Maugarny-Calès, A. and Laufs, P. (2018). Getting leaves into shape: A molecular, cellular, environmental and evolutionary view. Development 145: dev161646. https://doi.org/10.1242/dev.161646
Google Scholar: Author Only Title Only Author and Title

Melnyk, C.W., Schuster, C., Leyser, O., and Meyerowitz, E.M. (2015). A developmental framework for graft formation and vascular reconnection in Arabidopsis thaliana. Curr. Biol. 25: 1306–1318. https://doi.org/10.1016/j.cub.2015.03.032
Google Scholar: Author Only Title Only Author and Title

Nagpal, P., Ellis, C.M., Weber, H., Ploense, S.E., Barkawi, L.S., Guilfoyle, T.J., Hagen, G., Alonso, J.M., Cohen, J.D., Farmer, E.E., Ecker, J.R., and Reed, J.W. (2005). Auxin response factors ARF6 and ARF8 promote jasmonic acid production and flower maturation. Development 132: 4107–4118. https://doi.org/10.1242/dev.01955
Google Scholar: Author Only Title Only Author and Title

Nakayama, H., Nakayama, N., Seiki, S., Kojima, M., Sakakibara, H., Sinha, N., and Kimuraa, S. (2014). Regulation of the KNOX-GA gene module induces heterophyllic alteration in North American lake cress. Plant Cell 26: 4733–4748.

https://doi.org/10.1105/tpc.114.130229
Google Scholar: Author Only Title Only Author and Title

Nikovics, K., Blein, T., Peaucelle, A., Ishida, T., Morin, H., Aida, M., and Laufs, P. (2006). The balance between the MIR164A and CUC2 genes controls leaf margin serration in Arabidopsis. Plant Cell 18: 2929–2945. https://doi.org/10.1105/tpc.106.045617
Google Scholar: Author Only Title Only Author and Title

Ori, N. et al. (2007). Regulation of LANCEOLATE by miR319 is required for compound-leaf development in tomato. Nat. Genet. 39: 787–791. https://doi.org/10.1038/ng2036
Google Scholar: Author Only Title Only Author and Title

Pabõn-Mora, N., Sharma, B., Holappa, L.D., Kramer, E.M., and Litt, A. (2013). The Aquilegia FRUITFULL-like genes play key roles in leaf morphogenesis and inflorescence development. Plant J. 74: 197–212. https://doi.org/10.1111/tpj.12113
Google Scholar: Author Only Title Only Author and Title

Pastore, J.J., Limpuangthip, A., Yamaguchi, N., Wu, M.F., Sang, Y., Han, S.K., Malaspina, L., Chavdaroff, N., Yamaguchi, A., and Wagner, D. (2011). LATE MERISTEM IDENTITY2 acts together with LEAFY to activate APETALA1. Development 138: 3189–3198. https://doi.org/10.1242/dev.063073
Google Scholar: Author Only Title Only Author and Title

Pelaz, S., Tapia-López, R., Alvarez-Buylla, E.R., and Yanofsky, M.F. (2001). Conversion of leaves into petals in Arabidopsis. Curr. Biol. 11: 182–184. https://doi.org/10.1016/S0960-9822(01)00024-0
Google Scholar: Author Only Title Only Author and Title

Reeves, P.H. et al. (2012). A regulatory network for coordinated flower maturation. PLOS Genet. 8: e1002506. https://doi.org/10.1371/journal.pgen.1002506
Google Scholar: Author Only Title Only Author and Title

Rinne, P.L.H., Welling, A., Vahala, J., Ripel, L., Ruonala, R., Kangasjärvi, J., and van der Schoot, C. (2011). Chilling of dormant buds hyperinduces FLOWERING LOCUS T and recruits GA-inducible 1,3-β-glucanases to reopen signal conduits and release dormancy in Populus. Plant Cell 23: 130–146. https://doi.org/10.1105/tpc.110.081307
Google Scholar: Author Only Title Only Author and Title

Rodriguez, R.E., Debernardi, J.M., and Palatnik, J.F. (2014). Morphogenesis of simple leaves: regulation of leaf size and shape. Wiley Interdiscip. Rev. Dev. Biol. 3: 41–57. https://doi.org/10.1002/wdev.115
Google Scholar: Author Only Title Only Author and Title

Roeder, A.H.K., Chickarmane, V., Cunha, A., Obara, B., Manjunath, B.S., and Meyerowitz, E.M. (2010). Variability in the control of cell division underlies sepal epidermal patterning in Arabidopsis thaliana. PLoS Biol. 8: e1000367. https://doi.org/10.1371/journal.pbio.1000367
Google Scholar: Author Only Title Only Author and Title

Runions, A., Tsiantis, M., and Prusinkiewicz, P. (2017). A common developmental program can produce diverse leaf shapes. New Phytol. 216: 401–418. https://doi.org/10.1111/nph.14449
Google Scholar: Author Only Title Only Author and Title

Sablowski, R. (2015). Control of patterning, growth, and differentiation by floral organ identity genes. J. Exp. Bot. 66: 1065–1073. https://doi.org/10.1093/jxb/eru514
Google Scholar: Author Only Title Only Author and Title

Salem, M.A., Li, Y., Bajdzienko, K., Fisahn, J., Watanabe, M., Hoefgen, R., Schöttler, M.A., and Giavalisco, P. (2018). RAPTOR controls developmental growth transitions by altering the hormonal and metabolic balance. Plant Physiol. 177: 565–593. https://doi.org/10.1104/pp.17.01711
Google Scholar: Author Only Title Only Author and Title

Sapala, A. et al. (2018). Why plants make puzzle cells, and how their shape emerges. Elife 7: e32794. https://doi.org/10.7554/eLife.32794
Google Scholar: Author Only Title Only Author and Title

Sauret-Güeto, S., Schiessl, K., Bangham, A., Sablowski, R., and Coen, E. (2013). JAGGED controls arabidopsis petal growth and shape by interacting with a divergent polarity field. PLoS Biol. 11: e1001550. https://doi.org/10.1371/journal.pbio.1001550
Google Scholar: Author Only Title Only Author and Title

Schiessl, K., Kausika, S., Southam, P., Bush, M., and Sablowski, R. (2012). JAGGED controls growth anisotropy and coordination between cell size and cell cycle during plant organogenesis. Curr. Biol. 22: 1739–1746. https://doi.org/10.1016/j.cub.2012.07.020
Google Scholar: Author Only Title Only Author and Title

Schwarz, S., Grande, A. V., Bujdoso, N., Saedler, H., and Huijser, P. (2008). The microRNA regulated SBP-box genes SPL9 and SPL15 control shoot maturation in Arabidopsis. Plant Mol. Biol. 67: 183–195. https://doi.org/10.1007/s11103-008-9310-z
Google Scholar: Author Only Title Only Author and Title

Shani, E., Ben-Gera, H., Shleizer-Burko, S., Burko, Y., Weiss, D., and Ori, N. (2010). Cytokinin regulates compound leaf development in tomato. Plant Cell 22: 3206–3217. https://doi.org/10.1105/tpc.110.078253
Google Scholar: Author Only Title Only Author and Title

Shikata, M., Koyama, T., Mitsuda, N., and Ohme-Takagi, M. (2009). Arabidopsis SBP-Box genes SPL10, SPL11 and SPL2 control morphological change in association with shoot maturation in the reproductive phase. Plant Cell Physiol. 50: 2133–2145. https://doi.org/10.1093/pcp/pcp148
Google Scholar: Author Only Title Only Author and Title

Silveira, S.R., Le Gloanec, C., Gómez-Felipe, A., Routier-Kierzkowska, A-L.L., and Kierzkowski, D. (2022). Live-imaging provides an atlas of cellular growth dynamics in the stamen. Plant Physiol. 188: 769–781. https://doi.org/10.1093/plphys/kiab363
Google Scholar: Author Only Title Only Author and Title

Smyth, D.R., Bowman, J.L., and Meyerowitz, E.M. (1990). Early flower development in Arabidopsis. Plant Cell 2: 755–767. https://doi.org/10.1105/tpc.2.8.755
Google Scholar: Author Only Title Only Author and Title

Strauss, S. et al. (2022). Using positional information to provide context for biological image analysis with MorphoGraphX 2.0. Elife 11: e72601. https://doi.org/10.7554/eLife.72601
Google Scholar: Author Only Title Only Author and Title

Su, H., Abernathy, S.D., White, R.H., and Finlayson, S.A. (2011). Photosynthetic photon flux density and phytochrome B interact to regulate branching in Arabidopsis. Plant. Cell Environ. 34: 1986–1998. https://doi.org/10.1111/j.1365-3040.2011.02393.x
Google Scholar: Author Only Title Only Author and Title

Tang, H.-B., Wang, J., Wang, L., Shang, G.-D., Xu, Z.-G., Mai, Y.-X., Liu, Y.-T., Zhang, T.-Q., and Wang, J.-W. (2023). Anisotropic cell growth at the leaf base promotes age-related changes in leaf shape in Arabidopsis thaliana. Plant Cell 35: 1386–1407. https://doi.org/10.1093/plcell/koad031
Google Scholar: Author Only Title Only Author and Title

Vlad, D. et al. (2014). Leaf shape evolution through duplication, regulatory diversification and loss of a homeobox gene. Science 343: 780–783. https://doi.org/10.1126/science.1248384
Google Scholar: Author Only Title Only Author and Title

Vuolo, F. et al. (2018). LMI1 homeodomain protein regulates organ proportions by spatial modulation of endoreduplication. Genes Dev. 32: 1361–1366. https://doi.org/10.1101/gad.318212.118
Google Scholar: Author Only Title Only Author and Title

Wang, Y., Strauss, S., Liu, S., Pieper, B., Lymbouridou, R., Runions, A., and Tsiantis Correspondence, M. (2022). The cellular basis for synergy between RCO and KNOX1 homeobox genes in leaf shape diversity. Curr. Biol. 32: 3773-3784.e5. https://doi.org/10.1016/j.cub.2022.08.020
Google Scholar: Author Only Title Only Author and Title

Werner, S., Bartrina, I., Novák, O., Strnad, M., Werner, T., and Schmülling, T. (2021). The cytokinin status of the epidermis regulates aspects of vegetative and reproductive development in Arabidopsis thaliana. Front. Plant Sci. 12: 613488. https://doi.org/10.3389/fpls.2021.613488
Google Scholar: Author Only Title Only Author and Title

Whitewoods, C.D., Gonçalves, B., Cheng, J., Cui, M., Kennaway, R., Lee, K., Bushell, C., Yu, M., Piao, C., and Coen, E. (2020). Evolution of carnivorous traps from planar leaves through simple shifts in gene expression. Science 367: 91–96. https://doi.org/10.1126/science.aay5433
Google Scholar: Author Only Title Only Author and Title

Willis, L., Refahi, Y., Wightman, R., Landrein, B., Teles, J., Huang, K.C., Meyerowitz, E.M., and Jönsson, H. (2016). Cell size and growth regulation in the Arabidopsis thaliana apical stem cell niche. Proc. Natl. Acad. Sci. U. S. A. 113: E8238–E8246. https://doi.org/10.1073/pnas.1616768113
Google Scholar: Author Only Title Only Author and Title

Wu, W., Du, K., Kang, X., and Wei, H. (2021). The diverse roles of cytokinins in regulating leaf development. Hortic. Res. 8: 118. https://doi.org/10.1038/s41438-021-00558-3
Google Scholar: Author Only Title Only Author and Title

Xu, M., Hu, T., Zhao, J., Park, M.Y., Earley, K.W., Wu, G., Yang, L., and Poethig, R.S. (2016). Developmental functions of miR156-regulated SQUAMOSA PROMOTER BINDING PROTEIN-LIKE (SPL) genes in Arabidopsis thaliana. PLOS Genet. 12: e1006263. https://doi.org/10.1371/journal.pgen.1006263
Google Scholar: Author Only Title Only Author and Title

Yadav, A.S., Hong, L., Klees, P.M., Kiss, A., He, X., Barrios, I.M., Heeney, M., Galang, A.M.D., Smith, R.S., Boudaoud, A., and Roeder, A.H.K. (2023). Growth directions and stiffness across cell layers determine whether tissues stay smooth or buckle. bioRxiv. https://doi.org/10.1101/2023.07.22.549953

Google Scholar: Author Only Title Only Author and Title

Yang, M. and Jiao, Y. (2016). Regulation of axillary meristem initiation by transcription factors and plant hormones. Front. Plant Sci. 7. https://doi.org/10.3389/fpls.2016.00183

Google Scholar: Author Only Title Only Author and Title

Yu, S., Lian, H., and Wang, J.W. (2015). Plant developmental transitions: the role of microRNAs and sugars. Curr. Opin. Plant Biol. 27: 1–7. https://doi.org/10.1016/j.pbi.2015.05.009

Google Scholar: Author Only Title Only Author and Title

Žádníkova, P. et al. (2010). Role of PIN-mediated auxin efflux in apical hook development of Arabidopsis thaliana. Development 137: 607–617. https://doi.org/10.1242/dev.041277

Google Scholar: Author Only Title Only Author and Title

Zhang, Z., Runions, A., Mentink, R.A., Kierzkowski, D., Karady, M., Hashemi, B., Huijser, P., Strauss, S., Gan, X., Ljung, K., and Tsiantis, M. (2020). A WOX/auxin biosynthesis module controls growth to shape leaf form. Curr. Biol. 30: 4857-4868.e6. https://doi.org/10.1016/j.cub.2020.09.037

Google Scholar: Author Only Title Only Author and Title

Zhao, F. et al. (2020). Microtubule-mediated wall anisotropy contributes to leaf blade flattening. Curr. Biol. 30: 3972-3985.e6. https://doi.org/10.1016/j.cub.2020.07.076

Google Scholar: Author Only Title Only Author and Title